goat polyclonal anti-OSBP (Novus), rabbit polyclonal anti-TGN46 (*trans*-Golgi network protein 46 kDa; Sigma-Aldrich), and rabbit polyclonal anti-FLAG (Anaspec, San Jose, CA) to detect FLAG-tagged proteins. Coverslips were washed three times with PBS and once with antibody-binding buffer, followed by the incubation with corresponding secondary antibodies for the detection of primary antibodies. These were donkey antibodies against mouse (DyLight 488), rabbit (DyLight 549), and goat (DyLight 649; Rockland Immunochemicals, Gilbertsville, PA). The slides were analyzed by confocal laser scanning microscopy (Zeiss LSM 510), using 488-nm, 543-nm, and 633-nm laser lines. The nuclei were counterstained by DAPI (4′,6′-diamidino-2-phenylindole) (Invitrogen, Carlsbad, CA).

RESULTS

Identification of host factors associated with RNP complexes. To identify host factors involved in HCV RNA replication, we employed an affinity-based purification procedure to isolate RNP complexes under nondenaturing conditions. We inserted an affinity tag peptide called One-STrEP-tag (28 amino acid residues) in the C-terminal region of NS5A of subgenomic replicon constructs (see Fig. S1A in the supplemental material) and established stable replicon cell lines. This insertion did not interfere with the replication of HCV replicon RNA (see Fig. S1B in the supplemental material) and/or developing G418-resistant clones (see Fig. S1C in the supplemental material). We developed, a one-step, nondenaturing affinity column chromatography procedure for the isolation of NS5A-binding proteins or protein complexes. Purified protein complexes were analyzed by Western blot assay (see Fig. S2A and B in the supplemental material). Viral protein complexes purified by this method were subjected to proteomic MudPIT analysis, which revealed a large repertoire of cellular factors (see Tables S2 to S7 in the supplemental material) and included all the viral NS proteins. Western blot analysis of the isolated proteins demonstrated the association of host factors that were identified by proteomic analysis (see Fig. S2C, right panels, in the supplemental material). In this analysis, we chose proteins whose peptide spectrum counts were significantly high. Figure S2C in the supplemental material shows the association of ApoB, OSBP, adipose differentiation-related protein, and fatty acid synthase along with the representative HCV NS proteins, NS5A and NS3. In contrast, these proteins, including NS5A, were not detected in the eluted fractions prepared from wild-type replicon (without the One-STrEP-tag) lysates (see Fig. S2C, left panels, in the supplemental material). In this study, we focused on the association of OSBP and investigated its functional relevance in the cycles of HCV infection.

Downregulation of OSBP protein affects HCV replication and viral particle release. To demonstrate the functional role of this interaction, we employed RNA interference strategy. We developed lentiviral vectors encoding two OSBP-specific shRNAs (shRNA-1 and -2). These shRNAs have been previously reported to suppress OSBP mRNA synthesis effectively (31, 36). Huh7.5.1 cells were first infected with either of the lentiviral particle-encoding shRNAs and subsequently challenged with tissue culture-grown HCV particles at an MOI of 1. A lentivirus encoding a scrambled shRNA was used as a negative control. OSBP expression was monitored by Western blot assays (Fig. 1A) and by RT-PCR analysis (Fig. 1B). Cells expressing OSBP shRNA-1 and -2 displayed differential levels of suppression of OSBP protein (Fig. 1A, top). OSBP protein was barely detectable in shRNA-1-expressing cells. On the other hand, the reduction of OSBP was modest in shRNA-2-expressing cells. OSBP protein appears as a doublet representing differentially phosphorylated forms. Albumin levels were uniformly expressed in these lysates (Fig. 1A, second panel). We examined the expression of viral core and NS5A proteins, which reflected the profile of OSBP protein expression. Both viral proteins were barely detectable in shRNA-1-expressing cells, where OSBP proteins were severely depleted, indicating a functional role of OSBP in viral translation/replication. shRNA-2, on the other hand, modestly reduced their expression (Fig. 1, lower panels). We next performed quantitative RT-PCR analyses of OSBP mRNA and viral RNAs isolated from cellular extracts (intracellular) and culture supernatants (extracellular). Intracellular RNA levels indicate viral replication, whereas extracellular viral RNA is a measure of released viral particles in the culture supernatant. The results show that both shRNAs were effective in suppressing OSBP mRNA synthesis (63% and 53%, respectively, for shRNA-1 and -2) without affecting GAPDH mRNA levels (Fig. 1B and C). The unrelated scrambled shRNA (control) did not have any effect on OSBP mRNA synthesis (Fig. 1C). shRNA-1, which was more potent in silencing the OSBP mRNA (63% reduction) (Fig. 1B), significantly suppressed intracellular levels of HCV RNA (85% reduction) (Fig. 1D). shRNA-2, on the other hand, which caused a modest reduction of OSBP mRNA (53%) compared to the shRNA-1 (Fig. 1B), reduced the intracellular HCV RNA replication levels only modestly (14%) (Fig. 1D). When levels of extracellular virion RNA were analyzed, both shRNA-1 and -2 effectively blocked the release of viral particles in the culture medium (99.8% and 87.2% reduction, respectively) (Fig. 1E). More importantly, the shRNA-2, which has little effect on intracellular HCV RNA replication levels, dramatically reduced HCV release (Fig. 1E). We further confirmed these results by determining the number of focus-forming units of the cultured supernatant as described previously (58). The culture supernatant from HCV-infected cells, which was previously infected with lentiviral vector expressing scrambled (negative control) shRNA, yielded 6×10^4 focus-forming units per ml of supernatant, whereas supernatants from shRNA-1- and shRNA-2-expressing cells displayed significantly reduced infectious virion titers, indicating that OSBP depletion effectively attenuated the rate of infectious virion release (99.8% and 84.7%, respectively) (Fig. 1F). This result confirms the previous observation that shRNA-2, which does not affect HCV replication levels (intracellular levels), dramatically affected the accumulation of extracellular viral particles (Fig. 1, compare D with E and F). Taken together, these results indicate that OSBP expression is required for both viral replication and release of viral particles.

OSBP affects virus secretion. One of the unique characteristics of the OSBP protein is its ability to translocate to the Golgi apparatus upon ligand binding. The translocalization of OSBP is regulated by its PH domain, which binds to Golgi lipids such as PI4P (Fig. 2A). The RNA interference studies described above suggest that partial depletion of OSBP can cause inhibition of viral particle secretion. To elucidate the functional role of OSBP in virion maturation processes further, we generated several mutants of OSBP (Fig. 2B). These include an N-terminal region of OSBP containing only the PH domain fragment (N-PH), a deletion in the PH domain (ΔPH),

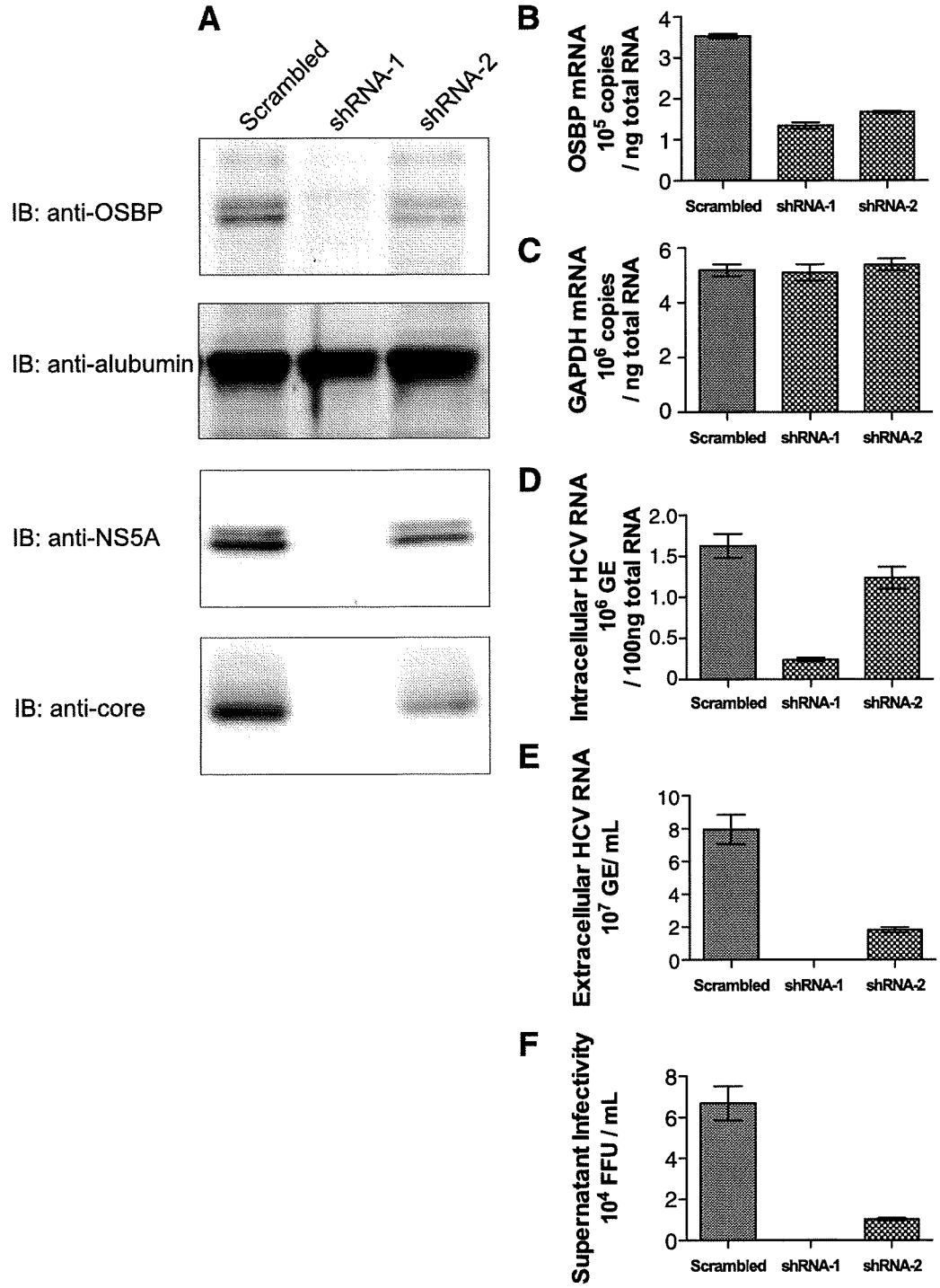

FIG. 1. Effect of silencing OSBP on HCV replication and viral particle release. Huh7.5.1 cells were infected with lentiviral vectors encoding an shRNA expression cassette of scrambled shRNA, shRNA-1, and shRNA-2. Four days after lentiviral infection, cells were infected with HCV (JFH1) at an MOI of 1. (A) Western blot analysis of HCV-infected cells with indicated shRNAs at day 6. IB, immunoblotting carried out using indicated antibodies. (B) Quantitative RT-PCR analysis of OSBP mRNA. (C) Quantitative RT-PCR analysis of GAPDH mRNA. (D) Intracellular HCV RNA levels measured by quantitative RT-PCR analysis. (E) Accumulation of extracellular HCV viral RNA in the culture medium as measured by quantitative RT-PCR analysis. (F) Supernatant infectivity assay. The infectivity of cultured supernatant at day 6 was determined as described in Materials and Methods and previously (58). Means and standard errors of at least triplicate measurements are shown. GE, genomic copies.

a base substitution mutation in the PH domain (W172A) (53), and mutation of FF to AA in the FFAT motif (FF/AA) (54) (Fig. 2B). Wild-type OSBP and the mutants were transiently transfected into Huh7 cells and analyzed for their subcellular distribution by indirect fluorescence microscopy using anti-FLAG antibody (OSBP and all OSBP mutants contain a FLAG tag at their N termini). Cells were counterstained with TGN46 antibody and DAPI. Both wild-type OSBP and the PH

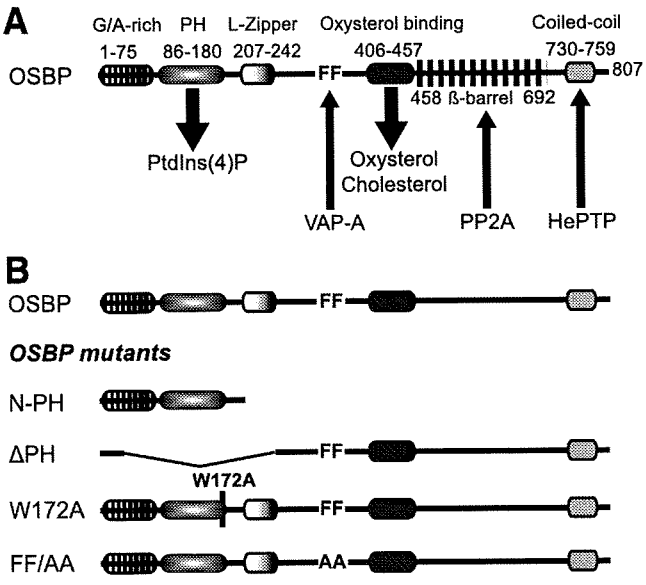

FIG. 2. Schematic representation of various OSBP domains. (A) The domain organizations of OSBP and amino acid regions are indicated on the figure. G/A-rich, glycine- and alanine-rich region; PH, binds to PI4P [PtdIns(4)P]; L-Zipper, leucine zipper domain; FF, FFAT; oxysterol-binding domain, binds to oxysterols and cholesterols. The numbering of amino acids is based on human OSBP (NM_002556). (B) OSBP mutants. The coding for the N-PH mutant extends from aa 1 to 208. The ΔPH mutant lacks aa 35 to 273. Mutant W172A carries a point mutation of a conserved tryptophan residue at 172 within the PH domain. Mutant FF/AA contains two phenylalanine residues in the FFAT motif replaced with alanine residues, required for VAP-A association. PP2A, phosphatase 2A; HePTP, tyrosine phosphatase.

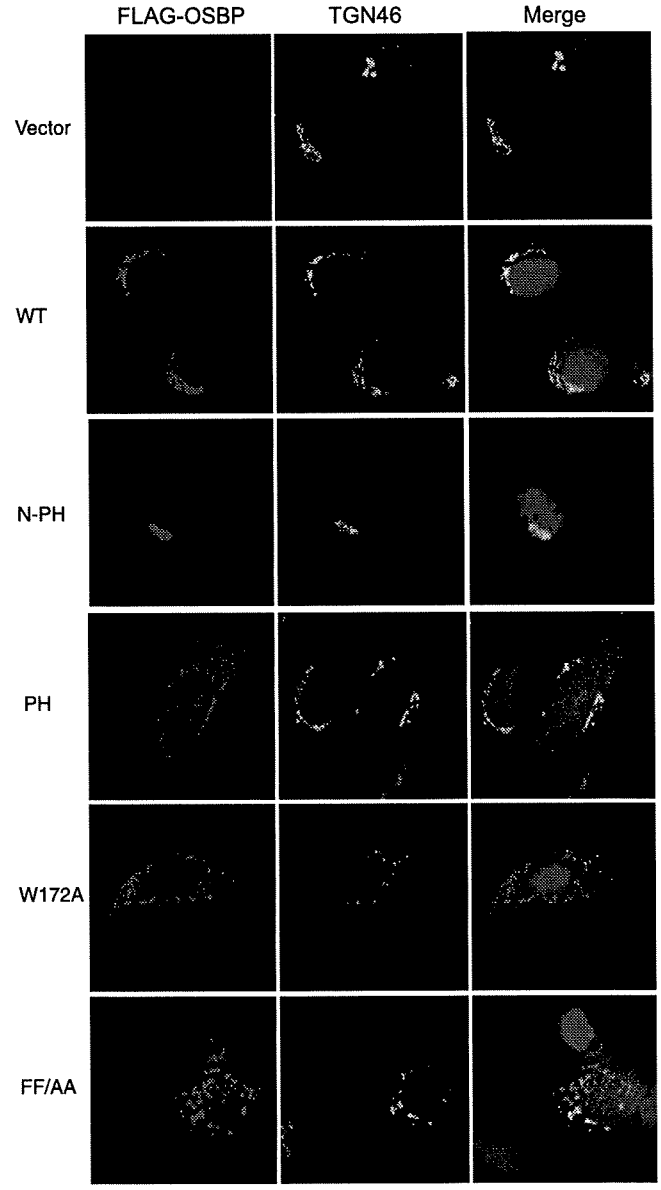

FIG. 3. Subcellular localization of OSBP and OSBP mutants. Huh7 cells were transfected with vectors encoding the FLAG-tagged wild-type (WT) and indicated mutant OSBP genes. Cells were analyzed by confocal immunofluorescence microscopy with anti-FLAG and anti-TGN46 antibodies (see Materials and Methods). Panels in the left column show FLAG-tagged OSBP (red). Panels in the center column show subcellular localization of TGN46 as a marker of the TGN. Panels in the right column show superimposed images of OSBP and TGN46.

domain-containing mutant (N-PH) predominantly localized to the Golgi compartment (Fig. 3). The N-PH mutant displayed Golgi compartment localizations as a consequence of its exposed PH domain. Other mutants including ΔPH and the base substitution mutants (W172A and FF/AA) in general displayed a diffuse cytosolic pattern of OSBP distribution. Both W172A and FF/AA mutants showed a punctate pattern of OSBP distribution in the cytosol and appeared to induce a distortion of TGN (Fig. 3). The OSBP mutant FF/AA displayed partial Golgi compartment localization. The substitutions of alanines for two phenylalanine residues in the FFAT motif abolish its ability to bind VAP-A (53, 54). VAP-A has been previously shown to bind NS5A (13, 17).

These OSBP mutants were also introduced into HCV-infected cells and examined for their effect on replication and viral particle release. Figure 4C shows a Western blot analysis of HCV-infected cells expressing ectopically expressed OSBP and its mutants. None of the OSBP mutants affected intracellular HCV RNA replication to any significant degree (Fig. 4B). However, the extracellular accumulation of viral RNA was affected by the ΔPH OSBP mutant (Fig. 4A). The PH domain is essential for the OSBP translocalization to the Golgi apparatus (24). Other mutants did not have any significant effect on the viral particle release except the W172A mutant. Surprisingly, the W172A mutant showed a modest increase in viral particle release. At present, we have no explanation for this observed result, but further characterization of this mutant will be needed. To further confirm the effect of OSBP mutants on HCV release, a chimeric HCV vector containing a luciferase reporter gene, analogous to Luc-Jc1 (23), was constructed and tested for virus production in the presence of OSBP mutants (Fig. 4D). Again, the ΔPH mutant consistently showed an inhibitory effect on viral particle release as assayed by luciferase activity of the released reporter virus. Based on these observations, the failure of the ΔPH OSBP mutant to maintain wild-type levels of viral particle release indicates that OSBP is

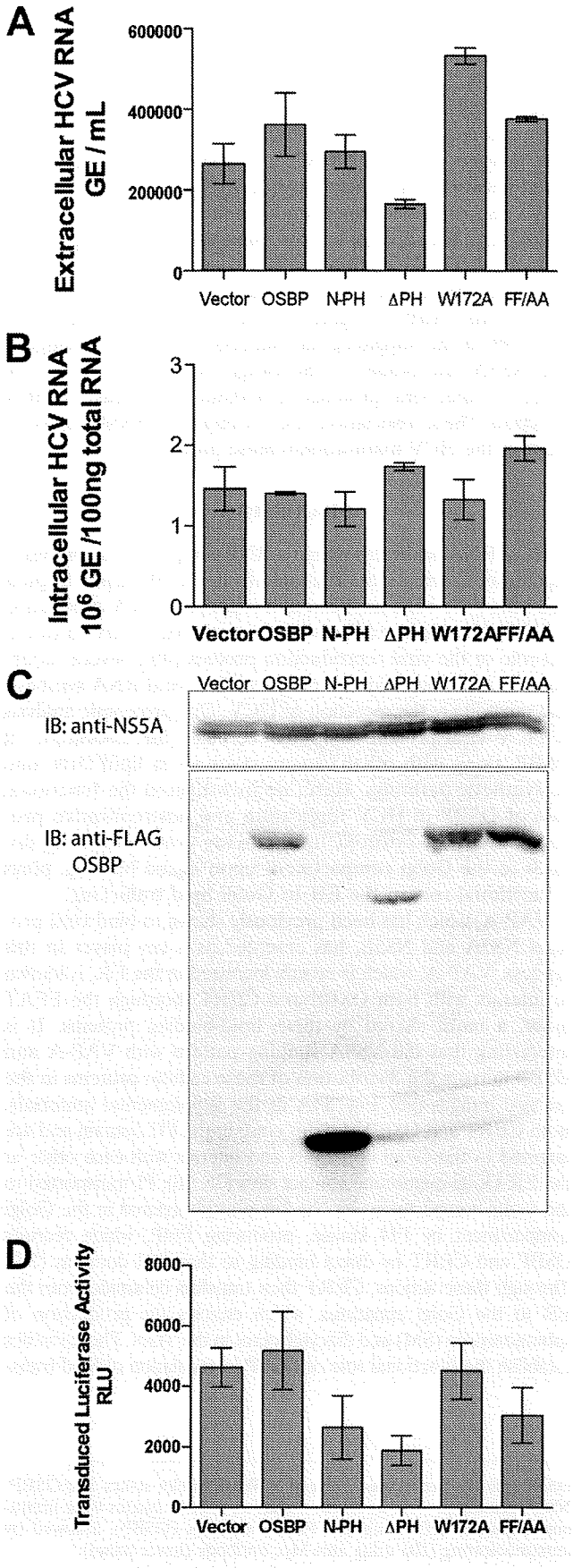

likely involved in viral particle release via the Golgi compartments.

NS5A binds OSBP. OSBP was identified in this study as an NS5A-associated protein (see Fig. S2C in the supplemental material). NS5A has been previously shown to interact with VAP-A and VAP-B (17). VAP-A also has been reported to bind OSBP (53). We have confirmed these interactions by immunoprecipitation studies. NS5A was shown to interact with OSBP and VAP-A (see Fig. S3A in the supplemental material). We further determined that OSBP interacts with NS5A irrespective of its genotypic origin. NS5A derived from genotype 1b (con1) or 2a (JFH1) binds to OSBP (see Fig. S3B in the supplemental material).

We next mapped the binding site(s) of OSBP within the NS5A protein. Huh7 cells were cotransfected with FLAG-tagged OSBP vector and various NS5A deletion mutants. All NS5A expression vectors contain a Myc/His tag (Fig. 5A). Cellular lysates were immunoprecipitated with anti-FLAG antibody to capture OSBP, followed by immunoblotting with anti-Myc antibody to probe for NS5A. Cellular lysates were examined for NS5A and OSBP expression by Western blot assays (Fig. 5B, upper and middle panels, respectively). The results show that N-terminal amino acid residues of NS5A in the region of amino acids (aa) 126 to 302 remained associated with OSBP (Fig. 5B, lower panel). These preliminary mapping studies identify domain I of NS5A as the approximate binding site(s) for OSBP. A more clearly defined motif of the NS5A region harboring OSBP binding needs to be identified. The interaction between NS5A and OSBP was also supported by the merged images of these proteins by confocal immunofluorescence microscopy, which displays a Golgi network-like pattern (see Fig. S4 in the supplemental material). The slightly diffuse pattern of OSBP seen here may reflect the state of the HCV-infected cell which may have contributed to the altered ER-Golgi apparatus pattern.

Oxysterol stimulates Golgi translocalization of OSBP and NS5A. 25-HC represents an oxidized sterol species and the most potent ligand for OSBP. The ligand binding to the OSBP triggers its Golgi translocalization, especially in the TGN. In Huh7 cells, the subcellular distribution of endogenous OSBP protein was cytosolic/vesicular as well as associated with the Golgi apparatus. OSBP association with the Golgi apparatus is seen as superimposed images in light blue (Fig. 6, top row).

FIG. 4. Effect of OSBP mutants on HCV replication and secretion. Huh7 cells were infected with HCV at an MOI of 0.5, maintained for 8 days, transfected with OSBP expression vector by electroporation, and analyzed after 48 h by RT-PCR (A and B) and Western blot assays (C). (A) Accumulation of HCV RNA in the culture supernatant. (B) The level of intracellular HCV RNA. (C) Western blot analysis of the HCV-infected cells using anti-NS5A (upper panel) and anti-FLAG for the detection of OSBP and mutants (lower panel). (D) Production of chimeric reporter HCV. Huh7.5.1 cells were transfected with both Luc-Jc1 RNA (luciferase reporter virus) and wild-type and mutant OSBP expression vectors, as indicated. Culture supernatants were collected at 72 h after transfection and used to infect naïve Huh7.5.1 cells. Cellular lysates from these secondary infections were assayed at 42 h for luciferase activity to determine the level of infectious reporter virion titer. Means and standard errors of at least triplicate measurements are shown. Expression vectors used for all the experiments are indicated. GE, genomic copies.

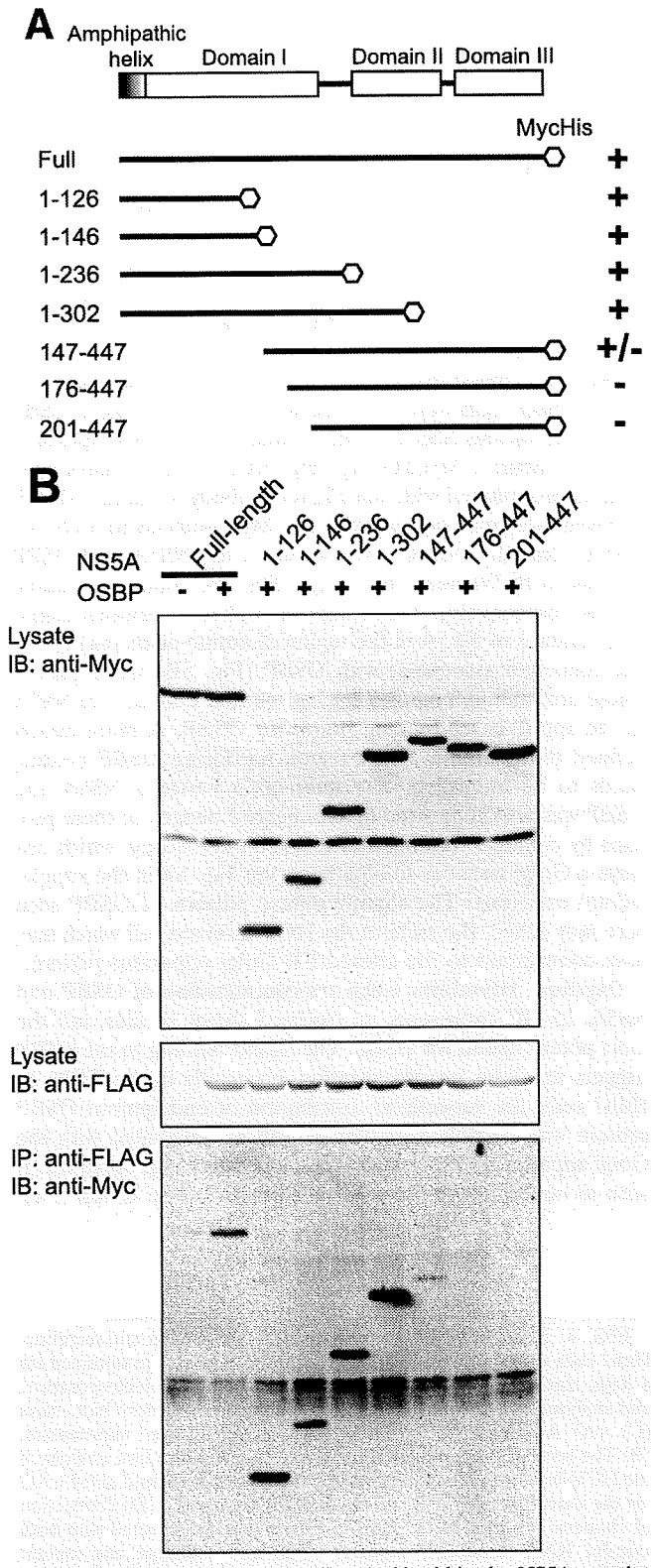

FIG. 5. Mapping of OSBP binding site(s) within the NS5A protein. (A) Schematic representation of wild-type and deletion mutants of NS5A encoded by pEF-NS5A vectors. Various domains of NS5A are shown. Huh7 cells were cotransfected with OSBP (pFLAG-CMV-OSBP), wild-type NS5A (pEF1-NS5A), or NS5A deletion mutants. Wild-type and mutant NS5A expression vectors contain a Myc/His tag. (B) Expression of wild-type NS5A, NS5A deletion mutant proteins (upper panel), and OSBP (middle panel) was analyzed by Western blot assays. For OSBP-NS5A protein-protein interaction studies, cellular lysates were immunoprecipitated (IP) using anti-FLAG antibody (OSBP), followed by immunoblotting (IB) using anti-Myc antibody (lower panel).

When Huh7 cells were stimulated by 25-HC, OSBP displayed a discrete and predominant Golgi compartment localization (Fig. 6, second row). When we analyzed the subcellular distribution of NS5A upon 25-HC stimulation in the HCV (JFH1)-infected cells, NS5A, in addition to its typical punctate ER localization, also displayed a discrete localization to the TGN. The merged image of OSBP and NS5A localization in the Golgi network can be seen in yellow (Fig. 6, bottom row).

We also examined this phenomenon in cells expressing the NS5A gene via an ectopic expression vector encoding NS5A. As can be seen, the addition of 25-HC again triggered its Golgi compartment distribution, suggesting that NS5A via its interaction with OSBP is targeted to the Golgi compartment (see Fig. S4B in the supplemental material). This result suggests that NS5A can localize to the Golgi compartment in the absence of other viral proteins or without the context of HCV infection. These associations clearly implicate NS5A's involvement in the HCV maturation/release processes.

DISCUSSION

HCV RNA replicates within a RNP complex in the modified membranous structures originated from the ER. Lipid droplets and rafts have been implicated in supporting HCV replication (13, 28). Host lipid synthesis has been shown to play an essential role in the viral reproduction process (40). Several inhibitors of lipid/fatty acid biosynthesis affect viral RNA synthesis and most likely the secretion of HCV. Our proteomic analysis of HCV viral protein complexes revealed the association of OSBP along with other factors involved in lipid/fatty acid biosynthetic pathways. Here, we investigated the functional role of OSBP in HCV replication and postreplicative processes. OSBP, a cytosolic lipid binding protein that translocates to the Golgi compartment upon ligand binding, plays a functional role in the ER to Golgi lipid trafficking.

VAP-A, which has been previously shown to bind viral proteins NS5A and NS5B, has emerged as a key player in this process. VAP-A, which is mostly localized in the ER, is known to interact with both OSBP and CERT thorough the FFAT motif, a motif shared by these lipid-binding proteins. It is interesting that the NS5A staining pattern with VAP-A and OSBP mirrors the distribution of these cellular proteins in the merged images (see Fig. S4A in the supplemental material). Both CERT and OSBP proteins contain the PH domain and are targeted to the Golgi apparatus and interact with each other at the ER-Golgi membrane contact sites (35, 36). PI transported to the Golgi compartment by Nir-2 is phosphorylated in the Golgi compartment by PI4 kinase, producing PI4P, which recruits OSBP and CERT by direct binding to their PH domains (35). Through these actions, CERT then transfers ceramide from the ER to the Golgi apparatus, which enables the production of sphingomyelin (SM) and diacylglycerol in the TGN. These studies establish the functional role of OSBP in regulation of lipid trans-

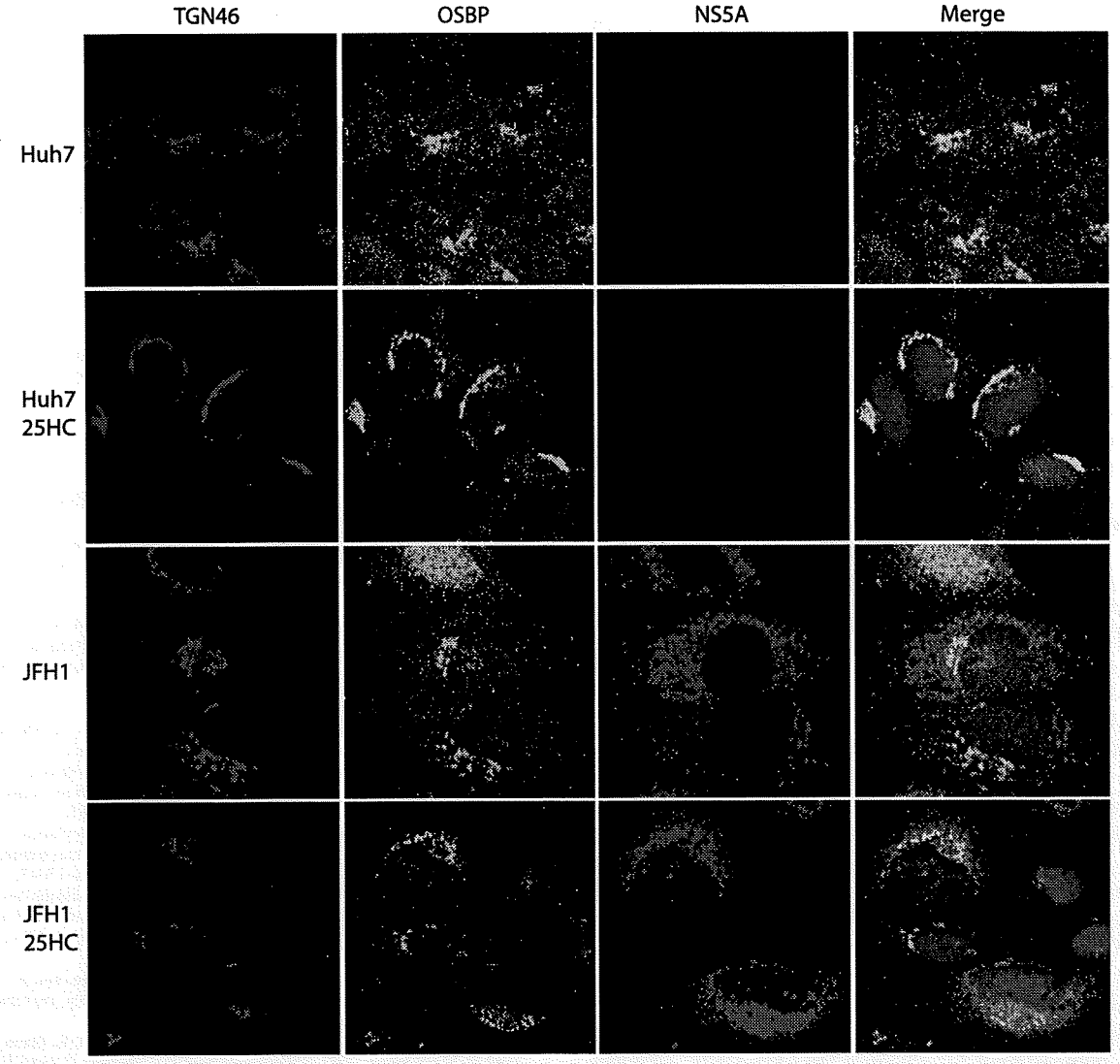

FIG. 6. 25-HC stimulates Golgi compartment localization of OSBP and NS5A. Uninfected and HCV (JFH1)-infected Huh7 cells were treated with or without 10 μM 25-HC and incubated for 12 h prior to immunostaining. The immunofluorescence assay was performed as described in Materials and Methods.

port from the ER to the Golgi apparatus and stimulation of SM synthesis. In this context, a recent study showed that HPA-12, an inhibitor SM synthesis, blocked HCV secretion, thus lending support to the model that HCV maturation/secretion may be occurring through the Golgi compartment (2). In this respect, two recent reports have demonstrated an indispensable role of PI4 kinases in HCV replication (4, 42).

Using RNA interference studies, it is shown that partial depletion of OSBP did not affect HCV replication but dramatically inhibited the accumulation of HCV particles (Fig. 1B to E). OSBP-specific shRNA-1, which severely depleted OSBP protein, affected both viral RNA replication and virion secretion. Such a depletion of OSBP by shRNA-1 also affected viral gene expression (Fig. 1A), suggesting that OSBP may be involved in the regulation of viral gene expression (translation/replication). The exact mechanism(s) by which this may occur remains to be characterized. Complete depletion of OSBP has been shown to cause Golgi apparatus fragmentation and inhibition of transport of vesicular stomatitis virus glycoprotein from the ER (30). Partial depletion of OSBP by shRNA-2 gave different results. The viral gene expression was proportionally affected by this shRNA (Fig. 1A). Intracellular levels of viral RNA were not affected, but the accumulation of extracellular RNA was severely reduced. This result suggested the involvement of OSBP in virion secretion.

Mutations within the functional domains of OSBP that affect its various functions have been described (50). We developed a few of these OSBP mutations and ectopically expressed them in HCV-infected cells (Fig. 2B). Most of these mutations displayed diffuse patterns of OSBP with reduced Golgi compartment localizations (W172A and FF/AA). The PH domain deletion mutant, ΔPH, failed to localize to the Golgi compartment, impairing the virion release (Fig. 1D and E). Overall, results of this study point more emphatically to a major role of OSBP in the regulation of virion secretion.

Several studies support the notion that HCV may utilize the

VLDL secretory pathway (6, 14, 19, 29). The most compelling evidence comes from the use of microsomal transfer protein inhibitor and ApoB silencing studies, both of which affect the VLDL particle assembly (14). Microsomal transfer protein inhibitor and ApoB small interfering RNA affect the accumulation of extracellular viral RNA while not affecting intracellular viral RNA replication (14). Use of the antioxidant flavonoid naringenin, which inhibits VLDL assembly, similarly inhibited virion release (29). Huang and colleagues showed that secretion of HCV infectious particles is dependent on active secretion of VLDL, showing that the VLDL assembly/secretion pathway is being utilized by HCV (19). Pre-VLDL particles are assembled in the ER, and mature VLDL particle formation occurs in the Golgi apparatus (16). While it is not known whether OSBP localization and/or trafficking to the Golgi apparatus is needed for VLDL secretion, we show here that NS5A along with OSBP is localized to the Golgi apparatus as well as to its characteristic localization in the ER. Our confocal microscopy studies show that a notable fraction of NS5A is localized to the Golgi compartment (Fig. 6). These data implicate a pivotal role of NS5A in a virion maturation process, which likely occurs in the Golgi compartments. NS5A interacts with OSBP via its N-terminal residues, and this interaction may be needed for NS5A's localization to the Golgi compartment as well. The preliminary data presented here map the binding site(s) of OSBP within domain I of NS5A (Fig. 4). Exact motifs involved in this interaction remain to be characterized. NS5A has three functional domains (I, II, and III). Domains I and II are relevant to the regulation of HCV RNA replication. Several studies point to the role of domain III in HCV particle secretion (3, 27, 45). The serine 457 residue in this domain, in particular, which is also the site of casein kinase II phosphorylation, has been shown to be essential for virion production (45). It will be of interest to determine the Golgi localization of an NS5A Ser^{457} mutant. The importance of Golgi trafficking for the HCV life cycle is further supported by the observations that HCV envelope proteins traffic thorough the cisternae of the Golgi compartment for glycosylation (32). Little is known about the HCV assembly and secretion processes. The studies described herein represent attempts to probe into these processes. Clearly, the delineation of these pathways is needed for the elucidation of the HCV life cycle and its relevance to infectious processes.

In summary, we have demonstrated that OSBP function(s) is relevant to the HCV maturation process. Our studies also suggest that NS5A localizes to the Golgi compartment and that OSBP and NS5A together aid in the viral assembly and or secretion processes. Further studies are needed to characterize, in depth, the exact role(s) of OSBP in the various steps of the HCV life cycle.

ACKNOWLEDGMENTS

We thank T. Wakita for the generous gift of the infectious JFH1 molecular clone and the subgenomic construct, F. Chisari (Scripps Research Institute, La Jolla, CA) for the kind gift of Huh7.5.1 cells, C. Rice and C. Cameron for anti-NS5A antibodies, I. Verma (Salk Institute, La Jolla, CA) for providing lentiviral plasmids, and Y. Matsuura for providing VAP-A expression vector.

This study was supported by NIH grants DK077704 and U19066313 to A.S. and P41 RR011823 to J.Y.

REFERENCES

1. **Ahlquist, P., A. O. Noueiry, W. M. Lee, D. B. Kushner, and B. T. Dye.** 2003. Host factors in positive-strand RNA virus genome replication. J. Virol. **77**:8181–8186.
2. **Aizaki, H., K. Morikawa, M. Fukasawa, H. Hara, Y. Inoue, H. Tani, K. Saito, M. Nishijima, K. Hanada, Y. Matsuura, M. M. Lai, T. Miyamura, T. Wakita, and T. Suzuki.** 2008. Critical role of virion-associated cholesterol and sphingolipid in hepatitis C virus infection. J. Virol. **82**:5715–5724.
3. **Appel, N., M. Zayas, S. Miller, J. Krijnse-Locker, T. Schaller, P. Friebe, S. Kallis, U. Engel, and R. Bartenschlager.** 2008. Essential role of domain III of nonstructural protein 5A for hepatitis C virus infectious particle assembly. PLoS Pathog. **4**:e1000035.
4. **Berger, K. L., J. D. Cooper, N. S. Heaton, R. Yoon, T. E. Oakland, T. X. Jordan, G. Mateu, A. Grakoui, and G. Randall.** 2009. Roles for endocytic trafficking and phosphatidylinositol 4-kinase III alpha in hepatitis C virus replication. Proc. Natl. Acad. Sci. USA **106**:7577–7582.
5. **Bern, M., D. Goldberg, W. H. McDonald, and J. R. Yates, 3rd.** 2004. Automatic quality assessment of peptide tandem mass spectra. Bioinformatics **20**(Suppl. 1):i49–i54.
6. **Chang, K. S., J. Jiang, Z. Cai, and G. Luo.** 2007. Human apolipoprotein e is required for infectivity and production of hepatitis C virus in cell culture. J. Virol. **81**:13783–13793.
7. **Chomczynski, P., and N. Sacchi.** 2006. The single-step method of RNA isolation by acid guanidinium thiocyanate-phenol-chloroform extraction: twenty-something years on. Nat. Protoc. **1**:581–585.
8. **Cociorva, D., L. T. D., and J. R. Yates.** 2007. Validation of tandem mass spectrometry database search results using DTASelect. Curr. Protoc. Bioinformatics Chapter **13**:Unit 13.4.
9. **Diop, S. B., K. Bertaux, D. Vasanthi, A. Sarkeshik, B. Goirand, D. Aragnol, N. S. Tolwinski, M. D. Cole, J. Pradel, J. R. Yates III, R. K. Mishra, Y. Graba, and A. J. Saurin.** 2008. Reptin and pontin function antagonistically with PcG and TrxG complexes to mediate Hox gene control. EMBO Rep. **9**:260–266.
10. **Elazar, M., K. H. Cheong, P. Liu, H. B. Greenberg, C. M. Rice, and J. S. Glenn.** 2003. Amphipathic helix-dependent localization of NS5A mediates hepatitis C virus RNA replication. J. Virol. **77**:6055–6061.
11. **Eng, J., A. McCormack, and J. R. Yates, 3rd.** 1994. An approach to correlate tandem mass spectral data of peptides with amino acid sequences in a protein database. J. Am. Soc. Mass Spectrom. **5**:976–989.
12. **Evans, M. J., C. M. Rice, and S. P. Goff.** 2004. Phosphorylation of hepatitis C virus nonstructural protein 5A modulates its protein interactions and viral RNA replication. Proc. Natl. Acad. Sci. USA **101**:13038–13043.
13. **Gao, L., H. Aizaki, J. W. He, and M. M. Lai.** 2004. Interactions between viral nonstructural proteins and host protein hVAP-33 mediate the formation of hepatitis C virus RNA replication complex on lipid raft. J. Virol. **78**:3480–3488.
14. **Gastaminza, P., G. Cheng, S. Wieland, J. Zhong, W. Liao, and F. V. Chisari.** 2008. Cellular determinants of hepatitis C virus assembly, maturation, degradation, and secretion. J. Virol. **82**:2120–2129.
15. **Gosert, R., D. Egger, V. Lohmann, R. Bartenschlager, H. E. Blum, K. Bienz, and D. Moradpour.** 2003. Identification of the hepatitis C virus RNA replication complex in Huh-7 cells harboring subgenomic replicons. J. Virol. **77**:5487–5492.
16. **Gusarova, V., J. Seo, M. L. Sullivan, S. C. Watkins, J. L. Brodsky, and E. A. Fisher.** 2007. Golgi-associated maturation of very low density lipoproteins involves conformational changes in apolipoprotein B, but is not dependent on apolipoprotein E. J. Biol. Chem. **282**:19453–19462.
17. **Hamamoto, I., Y. Nishimura, T. Okamoto, H. Aizaki, M. Liu, Y. Mori, T. Abe, T. Suzuki, M. M. Lai, T. Miyamura, K. Moriishi, and Y. Matsuura.** 2005. Human VAP-B is involved in hepatitis C virus replication through interaction with NS5A and NS5B. J. Virol. **79**:13473–13482.
18. **Huang, H., Y. Chen, and J. Ye.** 2007. Inhibition of hepatitis C virus replication by peroxidation of arachidonate and restoration by vitamin E. Proc. Natl. Acad. Sci. USA **104**:18666–18670.
19. **Huang, H., F. Sun, D. M. Owen, W. Li, Y. Chen, M. Gale, Jr., and J. Ye.** 2007. Hepatitis C virus production by human hepatocytes dependent on assembly and secretion of very low-density lipoproteins. Proc. Natl. Acad. Sci. USA **104**:5848–5853.
20. **Inubushi, S., M. Nagano-Fujii, K. Kitayama, M. Tanaka, C. An, H. Yokozaki, H. Yamamura, H. Nuriya, M. Kohara, K. Sada, and H. Hotta.** 2008. Hepatitis C virus NS5A protein interacts with and negatively regulates the non-receptor protein tyrosine kinase Syk. J. Gen. Virol. **89**:1231–1242.
21. **Kapadia, S. B., and F. V. Chisari.** 2005. Hepatitis C virus RNA replication is regulated by host geranylgeranylation and fatty acids. Proc. Natl. Acad. Sci. USA **102**:2561–2566.
22. **Kato, T., T. Date, M. Miyamoto, M. Sugiyama, Y. Tanaka, E. Orito, T. Ohno, K. Sugihara, I. Hasegawa, K. Fujiwara, K. Ito, A. Ozasa, M. Mizokami, and T. Wakita.** 2005. Detection of anti-hepatitis C virus effects of interferon and ribavirin by a sensitive replicon system. J. Clin. Microbiol. **43**:5679–5684.
23. **Koutsoudakis, G., A. Kaul, E. Steinmann, S. Kallis, V. Lohmann, T. Pietschmann, and R. Bartenschlager.** 2006. Characterization of the early steps

of hepatitis C virus infection by using luciferase reporter viruses. J. Virol. 80:5308–5320.
24. **Lagace, T. A., D. M. Byers, H. W. Cook, and N. D. Ridgway.** 1997. Altered regulation of cholesterol and cholesteryl ester synthesis in Chinese-hamster ovary cells overexpressing the oxysterol-binding protein is dependent on the pleckstrin homology domain. Biochem. J. 326:205–213.
25. **Levine, T. P., and S. Munro.** 2002. Targeting of Golgi-specific pleckstrin homology domains involves both PtdIns 4-kinase-dependent and -independent components. Curr. Biol. 12:695–704.
26. **MacCoss, M. J., C. C. Wu, and J. R. Yates, 3rd.** 2002. Probability-based validation of protein identifications using a modified SEQUEST algorithm. Anal. Chem. 74:5593–5599.
27. **Masaki, T., R. Suzuki, K. Murakami, H. Aizaki, K. Ishii, A. Murayama, T. Date, Y. Matsuura, T. Miyamura, T. Wakita, and T. Suzuki.** 2008. Interaction of hepatitis C virus nonstructural protein 5A with core protein is critical for the production of infectious virus particles. J. Virol. 82:7964–7976.
28. **Miyanari, Y., K. Atsuzawa, N. Usuda, K. Watashi, T. Hishiki, M. Zayas, R. Bartenschlager, T. Wakita, M. Hijikata, and K. Shimotohno.** 2007. The lipid droplet is an important organelle for hepatitis C virus production. Nat. Cell Biol. 9:1089–1097.
29. **Nahmias, Y., J. Goldwasser, M. Casali, D. van Poll, T. Wakita, R. T. Chung, and M. L. Yarmush.** 2008. Apolipoprotein B-dependent hepatitis C virus secretion is inhibited by the grapefruit flavonoid naringenin. Hepatology 47:1437–1445.
30. **Ngo, M., and N. D. Ridgway.** 2009. Oxysterol binding protein (OSBP)-related protein 9 (ORP9) is a cholesterol transfer protein that regulates Golgi structure and function. Mol. Biol. Cell 20:1388–1399.
31. **Nishimura, T., T. Inoue, N. Shibata, A. Sekine, W. Takabe, N. Noguchi, and H. Arai.** 2005. Inhibition of cholesterol biosynthesis by 25-hydroxycholesterol is independent of OSBP. Genes Cells 10:793–801.
32. **Op De Beeck, A., C. Voisset, B. Bartosch, Y. Ciczora, L. Cocquerel, Z. Keck, S. Foung, F. L. Cosset, and J. Dubuisson.** 2004. Characterization of functional hepatitis C virus envelope glycoproteins. J. Virol. 78:2994–3002.
33. **Pawlotsky, J. M.** 2004. Pathophysiology of hepatitis C virus infection and related liver disease. Trends Microbiol. 12:96–102.
34. **Peng, J., J. E. Elias, C. C. Thoreen, L. J. Licklider, and S. P. Gygi.** 2003. Evaluation of multidimensional chromatography coupled with tandem mass spectrometry (LC/LC-MS/MS) for large-scale protein analysis: the yeast proteome. J. Proteome Res. 2:43–50.
35. **Peretti, D., N. Dahan, E. Shimoni, K. Hirschberg, and S. Lev.** 2008. Coordinated lipid transfer between the endoplasmic reticulum and the Golgi complex requires the VAP proteins and is essential for Golgi-mediated transport. Mol. Biol. Cell 19:3871–3884.
36. **Perry, R. J., and N. D. Ridgway.** 2006. Oxysterol-binding protein and vesicle-associated membrane protein-associated protein are required for sterol-dependent activation of the ceramide transport protein. Mol. Biol. Cell 17:2604–2616.
37. **Randall, G., M. Panis, J. D. Cooper, T. L. Tellinghuisen, K. E. Sukhodolets, S. Pfeffer, M. Landthaler, P. Landgraf, S. Kan, B. D. Lindenbach, M. Chien, D. B. Weir, J. J. Russo, J. Ju, M. J. Brownstein, R. Sheridan, C. Sander, M. Zavolan, T. Tuschl, and C. M. Rice.** 2007. Cellular cofactors affecting hepatitis C virus infection and replication. Proc. Natl. Acad. Sci. USA 104: 12884–12889.
38. **Ridgway, N. D., P. A. Dawson, Y. K. Ho, M. S. Brown, and J. L. Goldstein.** 1992. Translocation of oxysterol binding protein to Golgi apparatus triggered by ligand binding. J. Cell Biol. 116:307–319.
39. **Sadygov, R. G., J. Eng, E. Durr, A. Saraf, H. McDonald, M. J. MacCoss, and J. R. Yates III.** 2002. Code developments to improve the efficiency of automated MS/MS spectra interpretation. J. Proteome Res. 1:211–215.
40. **Su, A. I., J. P. Pezacki, L. Wodicka, A. D. Brideau, L. Supekova, R. Thimme, S. Wieland, J. Bukh, R. H. Purcell, P. G. Schultz, and F. V. Chisari.** 2002. Genomic analysis of the host response to hepatitis C virus infection. Proc. Natl. Acad. Sci. USA 99:15669–15674.
41. **Tabb, D. L., W. H. McDonald, and J. R. Yates III.** 2002. DTASelect and Contrast: tools for assembling and comparing protein identifications from shotgun proteomics. J. Proteome Res. 1:21–26.
42. **Tai, A. W., Y. Benita, L. F. Peng, S. S. Kim, N. Sakamoto, R. J. Xavier, and R. T. Chung.** 2009. A functional genomic screen identifies cellular cofactors of hepatitis C virus replication. Cell Host Microbe 5:298–307.
43. **Takeuchi, T., A. Katsume, T. Tanaka, A. Abe, K. Inoue, K. Tsukiyama-Kohara, R. Kawaguchi, S. Tanaka, and M. Kohara.** 1999. Real-time detection system for quantification of hepatitis C virus genome. Gastroenterology 116:636–642.
44. **Targett-Adams, P., S. Boulant, and J. McLauchlan.** 2008. Visualization of double-stranded RNA in cells supporting hepatitis C virus RNA replication. J. Virol. 82:2182–2195.
45. **Tellinghuisen, T. L., K. L. Foss, and J. Treadaway.** 2008. Regulation of hepatitis C virion production via phosphorylation of the NS5A protein. PLoS Pathog 4:e1000032.
46. **Tiscornia, G., O. Singer, and I. M. Verma.** 2006. Design and cloning of lentiviral vectors expressing small interfering RNAs. Nat. Protoc. 1:234–240.
47. **van den Hoff, M. J., A. F. Moorman, and W. H. Lamers.** 1992. Electroporation in "intracellular" buffer increases cell survival. Nucleic Acids Res. 20:2902.
48. **Wakita, T., T. Pietschmann, T. Kato, T. Date, M. Miyamoto, Z. Zhao, K. Murthy, A. Habermann, H. G. Krausslich, M. Mizokami, R. Bartenschlager, and T. J. Liang.** 2005. Production of infectious hepatitis C virus in tissue culture from a cloned viral genome. Nat. Med. 11:791–796.
49. **Wang, P. Y., J. Weng, and R. G. Anderson.** 2005. OSBP is a cholesterol-regulated scaffolding protein in control of ERK 1/2 activation. Science 307: 1472–1476.
50. **Wang, P. Y., J. Weng, S. Lee, and R. G. Anderson.** 2008. The N terminus controls sterol binding while the C terminus regulates the scaffolding function of OSBP. J. Biol. Chem. 283:8034–8045.
51. **Waris, G., D. J. Felmlee, F. Negro, and A. Siddiqui.** 2007. Hepatitis C virus induces proteolytic cleavage of sterol regulatory element binding proteins and stimulates their phosphorylation via oxidative stress. J. Virol. 81:8122–8130.
52. **Waris, G., J. Turkson, T. Hassanein, and A. Siddiqui.** 2005. Hepatitis C virus (HCV) constitutively activates STAT-3 via oxidative stress: role of STAT-3 in HCV replication. J. Virol. 79:1569–1580.
53. **Wyles, J. P., C. R. McMaster, and N. D. Ridgway.** 2002. Vesicle-associated membrane protein-associated protein-A (VAP-A) interacts with the oxysterol-binding protein to modify export from the endoplasmic reticulum. J. Biol. Chem. 277:29908–29918.
54. **Wyles, J. P., and N. D. Ridgway.** 2004. VAMP-associated protein-A regulates partitioning of oxysterol-binding protein-related protein-9 between the endoplasmic reticulum and Golgi apparatus. Exp. Cell Res. 297:533–547.
55. **Yan, D., and V. M. Olkkonen.** 2008. Characteristics of oxysterol binding proteins. Int. Rev. Cytol. 265:253–285.
56. **Ye, J.** 2007. Reliance of host cholesterol metabolic pathways for the life cycle of hepatitis C virus. PLoS Pathog. 3:e108.
57. **Ye, J., C. Wang, R. Sumpter, Jr., M. S. Brown, J. L. Goldstein, and M. Gale, Jr.** 2003. Disruption of hepatitis C virus RNA replication through inhibition of host protein geranylgeranylation. Proc. Natl. Acad. Sci. USA 100:15865–15870.
58. **Zhong, J., P. Gastaminza, G. Cheng, S. Kapadia, T. Kato, D. R. Burton, S. F. Wieland, S. L. Uprichard, T. Wakita, and F. V. Chisari.** 2005. Robust hepatitis C virus infection in vitro. Proc. Natl. Acad. Sci. USA 102:9294–9299.

ARTICLE

Journal of Cellular Biochemistry 106:1123–1135 (2009)

Journal of Cellular Biochemistry

Identification of Annexin A1 as a Novel Substrate for E6AP-Mediated Ubiquitylation

Tetsu Shimoji,[1] Kyoko Murakami,[1] Yuichi Sugiyama,[1] Mami Matsuda,[1] Sachiko Inubushi,[2] Junichi Nasu,[1] Masayuki Shirakura,[1] Tetsuro Suzuki,[1] Takaji Wakita,[1] Tatsuya Kishino,[3] Hak Hotta,[2] Tatsuo Miyamura,[1] and Ikuo Shoji[1,2*]

[1]*Department of Virology II, National Institute of Infectious Diseases, Shinjuku-ku, Tokyo, Japan*

[2]*Division of Microbiology, Kobe University Graduate School of Medicine, Kobe, Hyogo, Japan*

[3]*Division of Functional Genomics, Center for Frontier Life Sciences, Nagasaki University, Nagasaki, Japan*

ABSTRACT

E6-associated protein (E6AP) is a cellular ubiquitin protein ligase that mediates ubiquitylation and degradation of p53 in conjunction with the high-risk human papillomavirus E6 proteins. However, the physiological functions of E6AP are poorly understood. To identify a novel biological function of E6AP, we screened for binding partners of E6AP using GST pull-down and mass spectrometry. Here we identified annexin A1, a member of the annexin superfamily, as an E6AP-binding protein. Ectopic expression of E6AP enhanced the degradation of annexin A1 in vivo. RNAi-mediated downregulation of endogenous E6AP increased the levels of endogenous annexin A1 protein. E6AP interacted with annexin A1 and induced its ubiquitylation in a Ca^{2+}-dependent manner. GST pull-down assay revealed that the annexin repeat domain III of annexin A1 is important for the E6AP binding. Taken together, our data suggest that annexin A1 is a novel substrate for E6AP-mediated ubiquitylation. Our findings raise the possibility that E6AP may play a role in controlling the diverse functions of annexin A1 through the ubiquitin-proteasome pathway. J. Cell. Biochem. 106: 1123–1135, 2009.

KEY WORDS: E6AP; ANNEXIN A1; UBIQUITIN; DEGRADATION

The ubiquitin/26S proteasome pathway plays important roles in the control of many basic cellular processes, such as cell cycle progression, signal transduction, transcriptional regulation, DNA repair, and the regulation of inflammation responses [Hershko and Ciechanover, 1998]. Ubiquitin is a 76-aa polypeptide that is highly conserved among eukaryotic organisms. The ubiquitin-proteasome pathway consists of an enzymatic cascade that ubiquitylates proteins, thereby targeting them for proteasomal degradation. The E1 ubiquitin-activating enzyme binds ubiquitin through a thioester linkage in an ATP-dependent manner [Ciechanover et al., 1981; Haas and Rose, 1982]. The activated ubiquitin is then transferred to the E2 ubiquitin-conjugating enzyme. E2 works in conjunction with the E3 ubiquitin-protein ligase, which is responsible for conferring substrate specificity [Hershko et al., 1986]. E3 mediates the transfer of ubiquitin to the target protein. The polyubiquitylated substrates are rapidly recognized and degraded by the 26S proteasome [Ciechanover, 1998; Ciechanover et al., 2000].

E6-associated protein (E6AP) was initially identified as the cellular factor that stimulates ubiquitin-dependent degradation of the tumor suppressor p53 in conjunction with the E6 protein of cervical cancer-associated human papillomavirus (HPV) types 16 and 18 [Huibregtse et al., 1993a; Scheffner et al., 1994]. The E6–E6AP complex functions as an E3 ubiquitin ligase in the ubiquitylation of p53 [Scheffner et al., 1993]. E6AP is the prototype of a family of ubiquitin ligases called HECT domain ubiquitin ligases, all of which contain a domain homologous to the

Abbreviations used: E6AP, E6-associated protein; HPV, human papillomavirus; MALDI-TOF, matrix assisted laser desorption ionization-time of flight; MS, mass spectrometry; HCV, hepatitis C virus; MAb, monoclonal antibody; PAb, polyclonal antibody; GAPDH, glyceraldehydes-3-phosphate dehydrogenase; CHX, cycloheximide.

T. Shimoji and K. Murakami contributed equally to this work.

Grant sponsor: Japan Health Sciences Foundation; Grant sponsor: Ministry of Health, Labor, and Welfare; Grant sponsor: Promotion of Fundamental Studies in Health Sciences of the National Institute of Biomedical Innovation (NIBIO), Japan.

*Correspondence to: Ikuo Shoji, MD, PhD, Division of Microbiology, Kobe University Graduate School of Medicine, 7-5-1 Kusunoki-cho, Chuo-ku, Kobe, Hyogo 650-0017, Japan. E-mail: ishoji@med.kobe-u.ac.jp

Received 26 November 2008; Accepted 14 January 2009 • DOI 10.1002/jcb.22096 • 2009 Wiley-Liss, Inc.

Published online 9 February 2009 in Wiley InterScience (www.interscience.wiley.com).

*E*6AP carboxyl *t*erminus [Huibregtse et al., 1995]. Known substrates of the E6–E6AP complex include the tumor suppressor p53 [Scheffner et al., 1993], the PDZ domain-containing protein scribble [Nakagawa and Huibregtse, 2000] and NFX1-91, a transcriptional repressor of the gene encoding hTERT [Gewin et al., 2004]. Interestingly, E6AP is not involved in the ubiquitylation of p53 in the absence of E6 [Talis et al., 1998]. Several potential E6-independent substrates for E6AP have been identified, such as HHR23A and HHR23B (the human orthologs of *Saccharomyces cerevisae* Rad23) [Kumar et al., 1999], Blk (a member of the Src family kinases) [Oda et al., 1999], Mcm7 (which is involved in DNA replication) [Kuhne and Banks, 1998], trihydrophobin 1 [Yang et al., 2007], and AIB1 (a steroid receptor coactivator) [Mani et al., 2006].

Some patients with Angelman syndrome, a severe neurological disorder linked to E6AP, have mutations within the catalytic cleft that have been shown to reduce E6AP ubiquitin ligase activity [Kishino et al., 1997; Cooper et al., 2004]. Despite the significant progress in the study of Angelman syndrome-associated E6AP mutations, none of the identified E6AP substrates have been directly linked to the disorder. The physiological functions of E6AP are poorly understood at present.

In an attempt to identify novel substrates of E6AP, we identified annexin A1 (formerly known as lipocortin 1) as an E6AP-binding protein. Annexin A1 is a 37-kDa member of the annexin superfamily of Ca^{2+} and phospholipid-binding proteins [Lim and Pervaiz, 2007]. Annexin A1 is involved in the inhibition of cell proliferation, anti-inflammatory effects, and the regulation of cell differentiation. In addition, annexin A1 is involved in the regulation of cell death signaling, phagocytosis of apoptosis, and the process of carcinogenesis [Buckingham et al., 2006; Lim and Pervaiz, 2007]. Annexin A1 is phosphorylated by various kinases such as tyrosine kinase, pp60c-src [Varticovski et al., 1988], protein kinase C [Oudinet et al., 1993], epidermal growth factor receptor protein kinase [Haigler et al., 1987], and hepatocyte growth factor receptor kinase [Skouteris and Schroder, 1996].

In this study, we have examined the possibility that the stability of annexin A1 is regulated through E6AP-dependent ubiquitylation. Our study revealed that E6AP mediates ubiquitin-dependent degradation of annexin A1 in a Ca^{2+}-dependent manner. Our results raise the possibility that E6AP may have a role in controlling the diverse functions of annexin A1.

MATERIALS AND METHODS

CELL CULTURE AND TRANSFECTION

Human embryonic kidney (HEK) 293T cells, and human cervical carcinoma C33-A cells were cultured in Dulbecco's modified Eagle's medium (DMEM) (Sigma, St. Louis, MO) supplemented with 50 IU/ml penicillin, 50 μg/ml streptomycin (Invitrogen, Carlsbad, CA), and 10% (v/v) fetal bovine serum (FBS) (JRH Biosciences, Lenexa, KS) at 37°C in a 5% CO_2 incubator. HEK 293T cells and C33-A cells were transfected with plasmid DNA using FuGene 6 transfection reagents (Roche, Mannheim, Germany). The *Spodoptera frugiperda* (Sf) 9 cells were cultured in TC100 (JRH Biosciences) supplemented with 10% (v/v) FBS and 100 μg/ml kanamycin at 26°C in an incubator. The *Trichoplusia ni* (Tn) 5 cells were cultured in Ex-Cell 405 (JRH Biosciences) at 26°C in an incubator.

PLASMIDS AND RECOMBINANT BACULOVIRUSES

To express annexin A1 as a FLAG-tagged fusion protein in mammalian cells, annexin A1 fragment was amplified from pKK-trc-lipo-155 (a kind gift from Dr. Browning, Biogen) by polymerase chain reaction (PCR) using two oligonucleotides, 5′-TATCCCGG-GAACCACCATGGCAATGGTATCAGAATTCC-3′ and 5′-TATGCGG-CCGCTTACTTATCGTCGTCATCCTTGTAATCGTTTCCTCCACAAAG-AGCC-3′. The FLAG-tag sequence was fused to the C-terminus of the annexin A1 gene in frame. The amplified PCR fragment was digested with *Sma*I and *Not*I, purified, and subcloned into pCAGGS [Niwa et al., 1991], resulting in pCAG-annexin A1-FLAG. To express E6AP and the active-site cysteine-to-alanine mutant of E6AP in mammalian cells, pCAG-HA-E6AP isoform II and pCAG-HA-E6AP C-A were used [Shirakura et al., 2007]. The C-A mutation was introduced at the site of E6AP C843 [Kao et al., 2000]. To express Nedd4, pCAG-HA-Nedd4 was constructed. To make a fusion protein consisting of glutathione S-transferase (GST) fused to the N-terminus of E6AP in *Escherichia coli* (*E. coli*), pGEX-E6AP was used [Shirakura et al., 2007]. Recombinant baculoviruses expressing GST-E6AP were described previously [Shirakura et al., 2007]. To express hexahistidine (His)-tagged annexin A1 in *E. coli*, annexin A1 fragment was amplified from pKK-trc-lipo-155 by PCR using two oligonucleotides, 5′-TATCCCGGGAACCACCATGGCAATGG-TATCAGAATTCC-3′ and 5′-ATAGCGGCCGCGTTTCCTCCACAAA-GAGCC-3′. The PCR fragment was purified and digested with *Sma*I and *Not*I. pET21b was digested with *Nde*I, blunt ended with a DNA blunting kit (Takara, Japan), and digested with *Not*I. Then, the PCR fragment of annexin A1 was ligated into the pET21b fragment, resulting in pET21b-annexin A1. To map the E6AP-binding site on annexin A1 protein, a series of expression plasmids for GST-annexin A1 fusion proteins were constructed by amplifying annexin A1 gene fragments with PCR using sense primers containing *Sma*I site and antisense primers containing a *Not*I site. The amplified PCR fragments were subcloned into pGEM T-Easy (Promega, Madison, WI) and verified by sequencing. Then, the annexin A1 gene fragments were digested with *Sma*I and *Not*I and ligated into the *Sma*I–*Not*I site of pGEX 4T-1 (GE Healthcare, Uppsala, Sweden). The annexin A1 (1-41) gene fragment was amplified from pET21b-annexin A1 by PCR using two oligonucleotides, 5′-TATCCCGG-GAACCACCATGGCAATGGTATCAGAATTCC-3′ and 5′-ATATAGC-GGCCGCTTAGGTAGGATAGGGGCTCACCGCT-3′. The PCR primers used to amplify the annexin A1 fragments were as follows:

Annexin A1 (42–346): 5′-TATCCCGGGAACCACCATGTTCAAT-CCATCCTCGGATGTCG-3′ and 5′-ATATAGCGGCCGCTTAGTTT-CCTCCACAAAGAGCC-3′.

Annexin A1 (42–113): 5′-AAACCCGGGTATGTTCAATCCATCCT-CGGATGTCG-3′ and 5′-TTTGCGGCCGCTTATTTTAGCAGAGC-TAAAACAAC-3′.

Annexin A1 (114–195): 5′-AAACCCGGGTATGACTCCAGCG-CAATTTGATGC-3′ and 5′-TTTGCGGCCGCTTAATTCACACCAA-AGTCCTCAG-3′.

Annexin A1 (196–274): 5′-AAACCCGGGTATGGAAGACTTGG-CTGATTCAG-3′ and 5′-TTTGCGGCCGCTTAGCTTGTGGCGCAC-TTCACG-3′.
Annexin A1 (275–346): 5′-AAACCCGGGTATGAAACCAGCTTT-CTTTGCAGAG-3′ and 5′-ATATAGCGGCCGCTTAGTTTCCTCCA-CAAAGAGCC-3′.
Annexin A1 (42–195): 5′-AAACCCGGGTATGTTCAATCCATCC-TCGGATGTCG-3′ and 5′-TTTGCGGCCGCTTAATTCACACCAAA-GTCCTCAG-3′.
Annexin A1 (114–274): 5′-AAACCCGGGTATGACTCCAGCGCA-ATTTGATGC-3′ and 5′-TTTGCGGCCGCTTAGCTTGTGGCGCAC-TTCACG-3′.
Annexin A1 (196–346): 5′-AAACCCGGGTATGGAAGACTTGG-CTGATTCAG-3′ and 5′-ATATAGCGGCCGCTTAGTTTCCTCCAC-AAAGAGCC-3′.

The sequences of the inserts were extensively verified using an ABI PRISM 3100-Avant Genetic Analyzer (Applied Biosystems, Foster City, CA). To express GST, GST-E6AP, and MEF-E6AP in the baculovirus expression system, recombinant baculoviruses were recovered using a BaculoGold transfection kit (Pharmingen, San Diego, CA) as described previously [Shirakura et al., 2007].

ANTIBODIES

The mouse monoclonal antibodies (MAbs) used in this study were anti-HA MAb (12CA5) (Roche), anti-HA 16B12 MAb (HA.11; BabCO), anti-Annexin I MAb (BD Biosciences, San Jose, CA), anti-glyceraldehyde-3-phosphate dehydrogenase (GAPDH) MAb (Chemicon, Temecula, CA), anti-GST MAb (Santa Cruz Biotechnology, Santa Cruz, CA), anti-ubiquitin MAb (Chemicon), anti-E6AP MAb (E6AP-330) (Sigma), and anti-β-actin MAb (Ab-1) (Calbiochem, San Diego, CA). The polyclonal antibodies (PAbs) used in this study were anti-HA rabbit PAb (Y-11; Santa Cruz Biotechnology), anti-FLAG rabbit PAb (F7425; Sigma), anti-E6AP rabbit PAb (H-182; Santa Cruz Biotechnology), and anti-GST goat PAb (Amersham Bioscience, Buckinghamshire, UK).

IDENTIFICATION OF E6AP-BINDING PROTEINS WITH MALDI-TOF MASS SPECTROMETRY

To screen for potential E6AP-binding proteins, GST pull-down assays were performed using GST-E6AP and ten 225 cm^2-flasks (Corning, New York, NY) of confluent C-33A cells as the source of protein. The cells were lysed in 15 ml of the cell lysis buffer (100 mM Tris–HCl, pH 7.4, 100 mM NaCl, 0.5% Triton X-100 [ICE Biomedicals, Aurora, OH], Complete protease inhibitor cocktail [Roche]). The samples were incubated at 4°C for 1 h, and centrifuged at 13,000*g* for 30 min. The supernatants were collected and pre-cleared with 250 μl of 50% slurry glutathione-Sepharose 4B beads (Amersham Bioscience) to remove proteins that can nonspecifically bind to glutathione-Sepharose 4B beads. The supernatants were then pre-cleared with 250 μg of GST immobilized on glutathione-Sepharose 4B beads to remove proteins which can bind to GST. Then, the supernatant was collected, mixed with 250 μg of GST-E6AP or GST immobilized on glutathione-Sepharose 4B beads, and incubated for 1 h at 4°C. The beads were collected and washed with the cell lysis buffer three times. To remove the bound proteins from GST-E6AP, the bound proteins were released with the releasing buffer (10 mM Tris–HCl, pH 7.4, 150 mM NaCl, 1% sodium deoxycholate, 0.1% sodium dodecyl sulfate [SDS], 1% Triton X-100) five times. The released proteins were mixed with 20% (w/v) trichloroacetic acid (TCA) and incubated at 4°C for 30 min. After centrifugation, the TCA-precipitated samples were washed with ice-cold acetone four times, dried, and lysed in SDS-polyacrylamide gel electrophoresis (SDS–PAGE) loading buffer. The samples were separated by 7.5% SDS–PAGE and stained with Coomassie brilliant blue (CBB). The specific protein bands were excised from the gel and subjected to in-gel trypsin digestion. The tryptic peptide mixtures were analyzed by MALDI-TOF/MS analysis [Kaji et al., 2000]. Prior to MALDI-TOF/MS analysis, the peptide mixtures were desalted using C18 Zip Tips (Millipore, Bedford, MA) according to the manufacturer's instructions. The peptide data were collected in the reflection mode and with positive polarity, using a saturated solution of α-cyano-4-hydroxycinnamic acid (Sigma) in 50% acetonitrile (PE Biosystems, Foster City, CA) and 0.1% trifluoroacetic acid as the matrix. Spectra were obtained using a Voyger DE-STR MALDI-TOF mass spectrometer (PE Biosystems). The database-fitting program MS-Fit at the website (http://jpsl.ludwig.edu.au/ucsfhtml3.4/msfit.htm) of the University of California, San Francisco was used to interpret the MS spectra of the protein digests.

EXPRESSION AND PURIFICATION OF RECOMBINANT PROTEINS

E. coli BL21 (DE3) cells were transformed with plasmids expressing GST fusion protein or His-tagged protein and grown at 37°C. Expression of the fusion protein was induced by 1 mM isopropyl-β-D-thiogalactopyranoside at 25°C for 4 h. Bacteria were harvested, suspended in lysis buffer (phosphate-buffered saline [PBS] containing 1% Triton X-100, Complete protease inhibitor cocktail, EDTA free [Roche]), and sonicated on ice.

Hi5 cells were infected with the recombinant baculoviruses to produce GST-E6AP or GST. GST-E6AP and GST-fusion proteins were purified on glutathione-Sepharose beads (Amersham Bioscience) according to the manufacturer's protocols. His-tagged proteins were purified on Ni-NTA beads (Qiagen, Hilden, Germany) according to the manufacturer's protocols. MEF-E6AP and MEF-E6AP C-A [Shirakura et al., 2007] were purified on anti-FLAG M2 agarose beads (Sigma) according to the manufacturer's protocols.

IMMUNOPRECIPITATION AND IMMUNOBLOT ANALYSIS

Cells were lysed in IP buffer (100 mM Tris–HCl, 100 mM NaCl, pH 7.4, 0.5% Triton X-100, 0.5 mM $CaCl_2$, plus Complete protease inhibitor cocktail, EDTA free) at 4°C for 15 min. Extracts were clarified by centrifugation at 13,000*g* for 20 min, and soluble lysates were pre-cleared with protein G Sepharose (GE Healthcare). The samples were incubated with anti-FLAG M2 agarose (Sigma) and rotated at 4°C for 5 h. The beads were washed five times with IP buffer, and bound proteins were eluted with Laemmli sample buffer. Samples were separated by 10% SDS–PAGE. Immunoblot analysis was performed essentially as described previously [Harris et al., 1999]. The membrane was visualized with SuperSignal West Pico Chemiluminescent Substrate (Pierce, Rockford, IL).

IN VIVO UBIQUITYLATION ASSAY

In vivo ubiquitylation assays were performed essentially as described previously [Shirakura et al., 2007]. Where indicated, cells were treated with 25 μM MG132 (Calbiochem) or with dimethylsulfoxide (DMSO; control) for 30 min prior to collection. FLAG-annexin A1 was immunoprecipitated with anti-FLAG MAb. Immunoprecipitates were analyzed by immunoblotting, using either anti-HA PAb or anti-annexin A1 MAb to detect ubiquitylated annexin A1.

IN VITRO UBIQUITYLATION ASSAY

In vitro ubiquitylation assays were performed essentially as described previously [Shirakura et al., 2007]. For in vitro ubiquitylation of annexin A1, purified GST-annexin A1 was used as a substrate. Purified GST was used as a negative control. Assays were done in 40-μl volumes containing 20 mM Tris–HCl, pH 7.6, 50 mM NaCl, 5 mM ATP, 8 μg of bovine ubiquitin (Sigma), 0.1 mM DTT, 200 ng of mouse E1, 200 ng of E2 (UbcH7), and 0.5 μg of MEF-E6AP, in the presence or absence of $CaCl_2$ as indicated. The reaction mixtures were incubated at 37°C for 120 min followed by immunoblotting.

SIRNA TRANSFECTION

HEK 293T cells (3×10^5 cells in a 6-well plate) were transfected with 40 pmol of either E6AP-specific small interfering RNA (siRNA; Sigma), or scramble negative-control siRNA duplexes (Sigma) using HiPerFect transfection reagent (Qiagen) following the manufacturer's instructions. The E6AP-siRNA target sequences were as follows:

siE6AP-1 (sense) 5′-GGGUCUACACCAGAUUGCUTT-3′; scramble negative control (siCont-1) (sense) 5′-UUGCGGGUCUAAUCACCGATT-3′ [Shirakura et al., 2007]; E6AP-2 (sense), 5′-CAACUCCUGCUCUGAGAUATT-3′; and scramble negative control (siCont-2), 5′-AGACCUACCCGAUUACUGUTT-3′ [Kelley et al., 2005].

ANNEXIN A1 PROTEIN AND E6AP-BINDING ASSAYS

To map the E6AP binding site on annexin A1 protein, GST pull-down assays were performed. A series of recombinant GST-annexin A1 proteins were expressed in *E. coli* and purified using glutathione-Sepharose 4B beads. Equivalent amounts of purified proteins, as estimated by CBB staining, were used for the binding assays. For pull-down assays, purified MEF-E6AP was incubated with GST-annexin A1 proteins immobilized on glutathione-Sepharose 4B beads in 1 ml of the binding buffer (50 mM Tris–HCl [pH 7.4], 150 mM NaCl, 1% Triton X-100, and 5 mM $CaCl_2$) at 4°C for 4 h. The beads were washed four times with binding buffer, and the pull-down complexes were separated by SDS–PAGE on 10% polyacrylamide gels and analyzed by immunoblotting with anti-FLAG MAb.

CYCLOHEXIMIDE (CHX) HALF-LIFE EXPERIMENTS

To examine the half-life of annexin A1 protein, transfected HEK 293T cells were treated with 50 μg/ml CHX at 44 h post-transfection. The cells at time-point zero were harvested immediately after treatment with CHX. Subsequent time points were incubated in medium containing CHX at 37°C for 3, 6, and 9 h as indicated.

CONFOCAL IMMUNOFLUORESCENCE MICROSCOPY

Cells were transfected with pCAG-HA-E6AP C-A and pCAG annexin A1-FLAG using TransIT-LT1 (Takara) according to the manufacturer's instructions. Transfected cells grown on collagen-coated coverslips were washed with PBS, fixed with 4% paraformaldehyde for 30 min at 4°C, and permeabilized with PBS containing 2% FCS and 0.3% Triton X-100. Cells were incubated with anti-HA mouse MAb and anti-FLAG rabbit PAb as primary antibodies, washed, and incubated with Alexa Fluor 488 goat anti-mouse IgG (Molecular Probes, Eugene, OR) and Alexa 555 Fluor goat anti-rabbit IgG (Molecular Probes) as secondary antibodies. Then the cells were washed with PBS, mounted on glass slides, and examined with an LSM510 laser scanning confocal microscope (Carl Zeiss, Oberkochen, Germany).

RESULTS

IDENTIFICATION OF ANNEXIN A1 AS A BINDING PARTNER FOR E6AP

To identify novel substrates for E6AP, we screened for E6AP-binding proteins using pull-down experiments with GST-E6AP. Whole cell lysates from C33-A cells were prepared as described above and incubated with immobilized GST-E6AP or GST alone. After the separation of bound proteins by SDS–PAGE, CBB staining of the gels revealed at least 15 specific bands precipitating with the GST-E6AP. The protein bands were excised from the gel and subjected to in-gel trypsin digestion. The tryptic peptide mixtures were analyzed by MALDI-TOF/MS as described above. Masses obtained using MALDI-TOF were analyzed using the MS-Fit program. This procedure identified seven individual proteins (Fig. 1A,a–g), such as a heat shock protein and a translation elongation factor. One of these bands, migrating at 37 kDa (Fig. 1A,e), was identified as annexin A1 based on six independent MS spectra (Fig. 1B). To verify the interaction of annexin A1 with E6AP, we repeated the pull-down experiments by incubating immobilized GST-E6AP with lysate from C-33A cells. Immunoblot analysis confirmed the proteomic identification of annexin A1 (Fig. 1C).

IN VIVO INTERACTION BETWEEN ANNEXIN A1 AND E6AP

To determine whether the interaction between annexin A1 and E6AP could take place in vivo, annexin A1-FLAG expression plasmid was introduced into HEK 293T cells together with either HA-E6AP expression plasmid or HA-Nedd4 (another HECT domain ubiquitin ligase) [Staub et al., 1996] expression plasmid. A catalytically inactive form of E6AP in which the active site cysteine residue has been substituted with alanine (C843A) was used to avoid potential degradation of interacting proteins. Cells were lysed and annexin A1-FLAG was immunoprecipitated with FLAG-beads. As shown in Figure 2A, HA-E6AP but not HA-Nedd4 was co-immunoprecipitated with annexin A1-FLAG, indicating that E6AP actually interacts with annexin A1 in the cells. We confirmed that the active form of HA-E6AP was also coimmunoprecipitated with annexin A1-FLAG (data not shown).

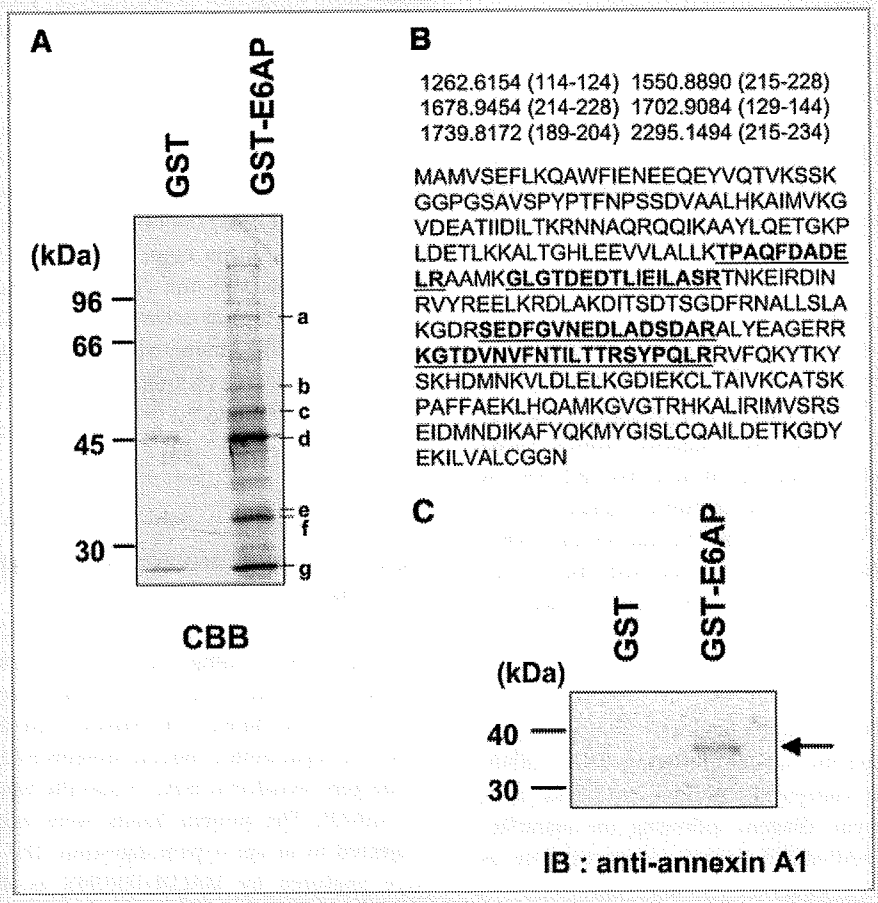

Fig. 1. Identification of annexin A1 as a binding partner for the E6AP. A: GST-E6AP on glutathione-Sepharose beads was incubated with whole-cell extract from C-33A cells. Bound proteins were detected by SDS-PAGE and CBB staining. Molecular weight markers are indicated, as well as the position of p37 (e), which likely corresponds to annexin A1. B: Peptide masses were identified by MALDI-TOF/MS and corresponding amino acids of annexin A1 (trypsin cleavage). Annexin A1 (accession no. 12654863) was identified through MALDI-TOF/MS as a candidate protein interacting with GST-E6AP. The database-fitting program MS-Fit was used to interpret the MS spectra of the protein digests. Six out of 22 masses obtained through the MALDI-TOF analysis corresponded to the theoretical values for annexin A1 cleavage (upper panel, amino acids corresponding to tryptic fragments in brackets) and represented 18% of the proteins' fragments (lower panel, peptides in bold print). The molecular weight search score, MOWSE, was 3.94E + 03. C: The identity of the band shown in panel A as annexin A1 was confirmed by Western blotting with anti-annexin A1 mouse MAb.

To determine whether annexin A1 and E6AP co-localize in the cells, immunofluorescence microscopy analysis was performed in two different cell lines, HEK 293T cells and C-33A cells. The immunofluorescence study showed that E6AP partially co-localized with annexin A1 in the cytoplasm of both types of cells (Fig. 2B).

To determine whether endogenous E6AP interacts with endogenous annexin A1 in vivo, C-33A cells were lysed and subjected to immunoprecipitation with anti-annexin A1 antibody or anti-E6AP antibody. Endogenous E6AP was co-immunoprecipitated with anti-annexin A1 antibody, but not with control antibody (Fig. 2C, left panel, upper lane). Moreover, endogenous annexin A1 was co-immunoprecipitated with anti-E6AP antibody, but not with control antibody (Fig. 2C, right panel, lower lane). These results suggest that endogenous E6AP can interact with endogenous annexin A1 in C-33A cells.

E6AP DECREASES STEADY-STATE LEVELS OF ANNEXIN A1 PROTEIN

To determine whether E6AP functions as an E3 ubiquitin ligase for the ubiquitylation of annexin A1, we assessed the effects of E6AP on annexin A1 protein in HEK 293T cells. The annexin A1-FLAG expression plasmid together with the plasmid for HA-tagged wild-type E6AP, catalytically inactive mutant E6AP, E6AP C-A, or Nedd4, was introduced into HEK 293T cells, and the levels of annexin A1 proteins were examined by immunoblotting. The steady-state levels of annexin A1 protein decreased with an increase of the E6AP plasmids (Fig. 3A,B). However, neither E6AP C-A nor Nedd4 decreased the steady-state levels of the annexin A1 protein, suggesting that E6AP enhances the degradation of annexin A1 protein.

E6AP ENHANCES THE DEGRADATION OF ANNEXIN A1 PROTEIN

To determine whether the E6AP-induced reduction of the annexin A1 protein is due to an increase in the rate of degradation of annexin A1 protein, we examined the degradation of annexin A1 using the protein synthesis inhibitor CHX. Annexin A1 together with wild-type E6AP or inactive mutant E6AP C-A was expressed in HEK 293T cells. At 44 h after transfection, the cells were treated with either 50 μg/ml CHX alone or 50 μg/ml CHX plus 25μM MG132 to inhibit

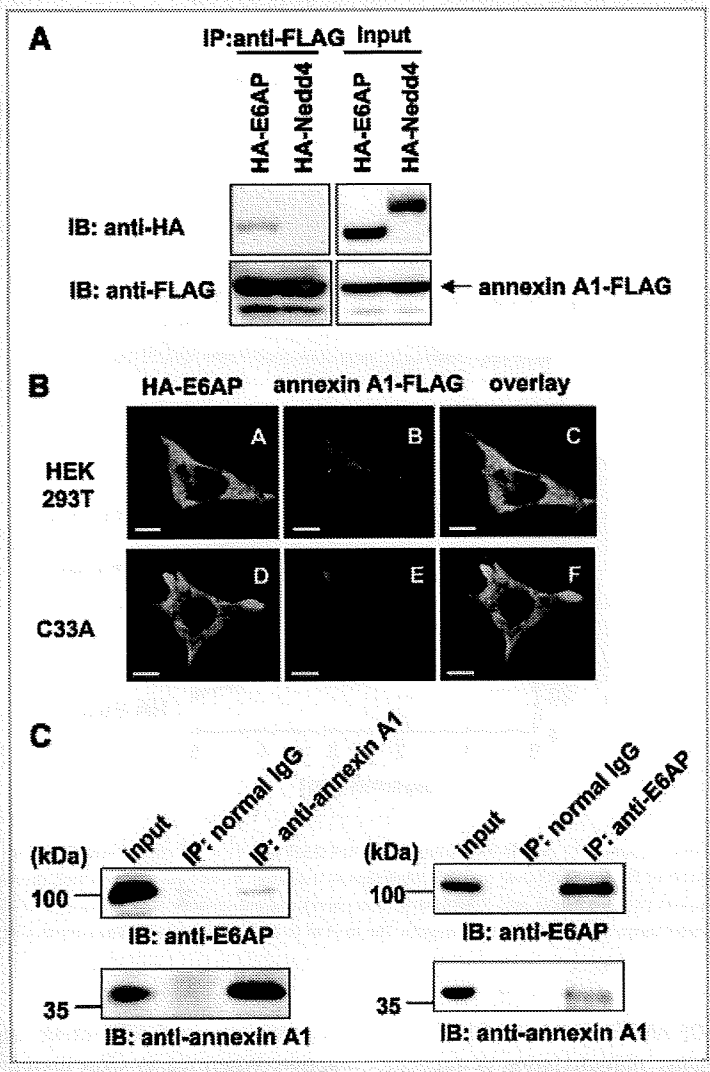

Fig. 2. In vivo interaction between annexin A1 and E6AP. A: HEK 293T cells were co-transfected with pCAG-annexin A1-FLAG together with pCAG-HA-E6AP C-A or pCAG-HA-Nedd4. The cell lysates were immunoprecipitated with FLAG beads and analyzed by immunoblotting with anti-HA PAb or anti-FLAG PAb. B: HEK 293T cells and C-33A cells were transfected with either HA-E6AP plasmid or annexin A1-FLAG plasmid, grown on coverslips, fixed, and processed for double-label immunofluorescence for HA-E6AP or annexin A1-FLAG. All the samples were examined with an LSM510 laser scanning confocal microscope (bar, 10 μm). C: C33A cells were lysed in the cell lysis buffer. The cell lysates were immunoprecipitated with anti-annexin A1 mouse MAb or control normal mouse IgG and analyzed with anti-E6AP mouse mAb or anti-annexin A1 mouse MAb as indicated (left panel). The cell lysates were immunoprecipitated with anti-E6AP mouse mAb or control normal mouse IgG and analyzed with anti-E6AP mouse mAb or anti-annexin A1 mouse mAb as indicated (right panel).

proteasome function. Cells were collected at 0, 3, 6, and 9 h following the treatment and analyzed by immunoblotting (Fig. 4A). Overexpression of E6AP resulted in rapid degradation of the annexin A1 protein, whereas the annexin A1 protein was stable in the cells transfected with inactive mutant E6AP C-A. Treatment of the cells with MG132 inhibited the degradation of annexin A1 (Fig. 4A). These results suggest that E6AP enhances proteasomal degradation of annexin A1.

KNOCKDOWN OF ENDOGENOUS E6AP BY SIRNA RESULTS IN ACCUMULATION OF ENDOGENOUS ANNEXIN A1 PROTEIN

To determine whether or not E6AP is critical for the degradation of endogenous annexin A1 protein, the expression of E6AP was knocked down by siRNA and the expression of annexin A1 and E6AP was analyzed by immunoblotting. We used two different siE6AP duplexes, siE6AP-1 and siE6AP-2, to knockdown the endogenous E6AP. Transfection of either siE6AP-1 or siE6AP-2 into HEK 293T cells resulted in a decrease in E6AP levels by 70–95% (Fig. 4B, the first panel), indicating that both siRNAs against E6AP resulted in a remarkable decrease in the protein level of E6AP. Knockdown of endogenous E6AP resulted in an accumulation of the endogenous annexin A1 protein, but no accumulation of the endogenous annexin A2 protein (Fig. 4B, the second and third panels), suggesting that the ubiquitylation and degradation of endogenous annexin A1 is specifically inhibited by knockdown of endogenous E6AP in vivo. These results suggest that endogenous E6AP plays a role in the proteolysis of endogenous annexin A1.

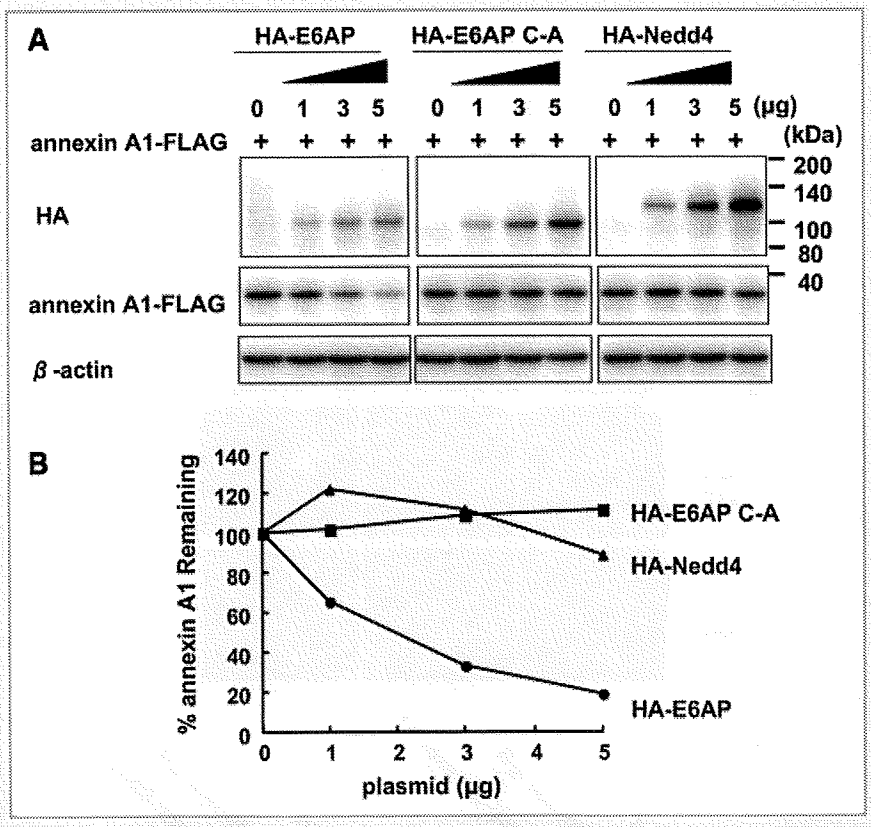

Fig. 3. E6AP decreases steady-state levels of annexin A1 protein in HEK 293T cells. HEK 293T cells (1×10^6 cells/10-cm dish) were transfected with 1 μg of pCAG annexin A1-FLAG along with either pCAG-HA-E6AP, pCAG-HA-E6AP C-A, or pCAG-HA-Nedd4 as indicated. At 48 h post-transfection, protein extracts were separated by SDS-PAGE and analyzed by immunoblotting with anti-HA PAb (top panel), anti-FLAG MAb (middle panel), and anti-β-actin MAb (bottom panel). B: Quantitation of data shown in panel A. Intensities of the gel bands were quantitated using the NIH Image 1.62 program. The level of β-actin served as a loading control. Circles, E6AP; squares, E6AP C-A; triangles, Nedd4.

E6AP MEDIATES UBIQUITYLATION OF ANNEXIN A1 IN VIVO

To determine whether E6AP can induce ubiquitylation of annexin A1 in cells, we performed in vivo ubiquitylation assays. HEK 293T cells were transfected with annexin A1-FLAG plasmid and either E6AP or Nedd4 plasmid, together with a plasmid encoding HA-tagged ubiquitin to facilitate the detection of ubiquitylated annexin A1 protein. Cell lysates were immunoprecipitated with anti-FLAG MAb and immunoblotted with anti-HA PAb to detect ubiquitylated annexin A1 protein. Only a faint ubiquitin signal was detected in the cells co-transfected with empty plasmid or Nedd4 plasmid (Fig. 5A, lanes 4 and 6). In contrast, co-expression of E6AP led to readily detectable ubiquitylated forms of the annexin A1 as a smear of higher-molecular-weight bands (Fig. 5A, lane 5). Immunoblot analysis with anti-FLAG PAb confirmed that annexin A1-FLAG proteins were immunoprecipitated and that higher-molecular-weight bands conjugated with HA-ubiquitin were indeed ubiquitylated forms of the annexin A1 proteins (Fig. 5B, lane 5). These results suggest that E6AP enhances ubiquitylation of annexin A1 in the cells.

E6AP MEDIATES UBIQUITYLATION OF ANNEXIN A1 IN VITRO

To reconstitute the E6AP-mediated ubiquitylation of annexin A1 in vitro, we performed an in vitro ubiquitylation assay of the annexin A1 using purified MEF-E6AP and GST-annexin A1 as described above. When the in vitro ubiquitylation reaction was carried out either in the absence of MEF-E6AP or in the presence of MEF-E6AP C-A, no ubiquitylation signal was detected (Fig. 5C, lanes 4 and 5). However, inclusion of purified MEF-E6AP in the reaction mixture resulted in ubiquitylation of GST-annexin A1 (Fig. 5C, lane 6), while no ubiquitylation was observed in the absence of ATP (Fig. 5C, lane 7). No signal was detected when GST was used as a substrate (data not shown). These results indicate that E6AP directly mediates ubiquitylation of annexin A1 protein in an ATP-dependent manner.

Ca^{2+}-DEPENDENT INTERACTION BETWEEN ANNEXIN A1 AND E6AP

We next assessed the effects of Ca^{2+} on the interaction between annexin A1 and E6AP. We performed the pull-down experiments by incubating immobilized GST-E6AP or GST alone with purified His-tagged annexin A1 in the presence or absence of 1 mM $CaCl_2$. After precipitation and SDS-PAGE, the bound annexin A1 was detected by immunoblotting with anti-annexin A1 antibody. GST-E6AP, but not GST, was able to precipitate annexin A1 only in the presence of Ca^{2+} (Fig. 6A, lane 4). These interactions were dependent on the concentration of Ca^{2+}, as increasing concentrations of Ca^{2+} resulted in an increase of binding of annexin A1 to E6AP (Fig. 6B). These

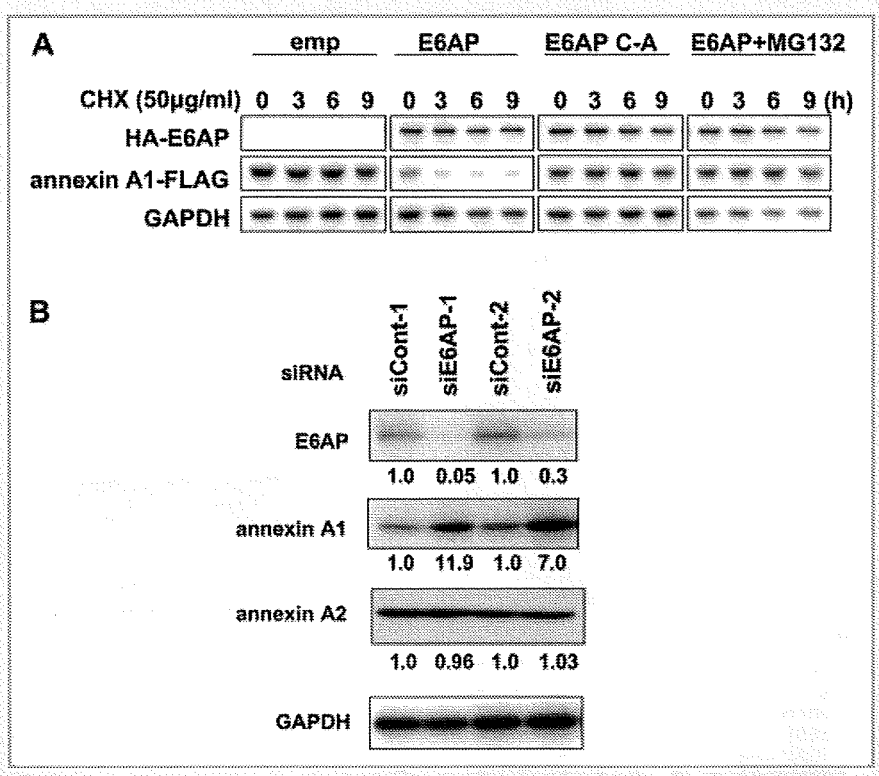

Fig. 4. E6AP-dependent degradation of annexin A1 protein. A: HEK 293T cells (1×10^6 cells/10-cm dish) were transfected with 1 μg of pCAG-annexin A1-FLAG plus 4 μg of empty vector, pCAG-HA-E6AP, or pCAG-HA-E6AP C-A. The cells were treated with 50 μg/ml CHX at 44 h after transfection. Cell extracts were collected at 0, 3, 6, and 9 h after treatment with CHX, followed by immunoblotting. Data are representative of three independent experimental determinations. B: Knockdown of endogenous E6AP by siRNA resulted in the accumulation of endogenous annexin A1 in HEK 293T cells. HEK 293T cells (3×10^5 cells/6-well plate) were transfected with 40 pmol of E6AP-specific duplex siRNA (or scramble negative control). Two sets of siRNAs (siE6AP-1 and siCont-1, siE6AP-2 and siCont-2) were used as described in Materials and Methods Section. The cells were harvested at 120 h after siRNA transfection. The relative levels of protein expression were quantitated using the NIH Image 1.62 program and are indicated below in the respective lanes. Data are representative of three independent experimental determinations.

results indicate that E6AP binds annexin A1 in a Ca^{2+}-dependent manner.

UBIQUITYLATION OF ANNEXIN A1 BY E6AP IS CA^{2+}-DEPENDENT

The HECT-type ubiquitin ligases transfer ubiquitin molecules to the substrates through direct interaction. Therefore, the E6AP-annexin A1 interaction is considered to be necessary for E6AP-mediated annexin A1 ubiquitylation. To determine if the molecular interaction is required for E6AP-mediated annexin A1 ubiquitylation, we performed in vitro ubiquitylation assay in the presence or absence of 1 mM $CaCl_2$. When in vitro ubiquitylation reaction was carried out in the presence of Ca^{2+}, the higher-molecular-weight species of GST-annexin A1 were detected with anti-GST PAb (Fig. 6C, lane 2), indicating that annexin A1 is polyubiquitylated by E6AP in vitro. However, no ubiquitylation signal was detected when the ubiquitylation reaction was carried out in the absence of Ca^{2+} (Fig. 6C, lane 1), indicating that the E6AP-annexin A1 interaction is required for E6AP-mediated annexin A1 ubiquitylation.

To further investigate whether the ubiquitylation of annexin A1 is dependent on the presence of Ca^{2+}, we examined the effects of EGTA on the E6AP-mediated ubiquitylation of annexin A1. Polyubiquitin chains were synthesized even in the presence of a high concentration of EGTA (Fig. 6D), indicating that E6AP was active even in the presence of EGTA. However, increasing amounts of EGTA resulted in decreases in the ubiquitylation of annexin A1 (Fig. 6E), suggesting that chelating the Ca^{2+} in the reaction mixture with EGTA inhibits the ubiquitylation of annexin A1. These findings suggest that the ubiquitylation of annexin A1 by E6AP is dependent on the presence of Ca^{2+}.

E6AP-BINDING DOMAIN FOR ANNEXIN A1 PROTEIN

To map the E6AP-binding domain on annexin A1 protein, GST pull-down assays were performed using a panel of annexin A1 deletion mutants expressed as GST-fusion proteins. Figure 7A shows a schematic representation of annexin A1 and known motifs in annexin A1. A series of deletion mutants of annexin A1 as GST fusion proteins (Fig. 7A) were expressed in *E. coli*. Purified MEF-E6AP was used to determine E6AP-binding domain. GST pull-down assays revealed that the core domain of annexin A1 (42-346), but not the N-terminal tail of annexin A1 (1-41), bound to E6AP (Fig. 7B, lanes 4 and 3). GST pull-down assays also showed that annexin A1 (114-274) and annexin A1 (196-346), but not annexin A1 (42-195), were able to bind to E6AP (Fig. 7B, lanes 5-7). As shown in Fig. 7C, GST-annexin A1 (196-274) bound to E6AP. These findings suggest that annexin repeat domain III is important for E6AP binding.

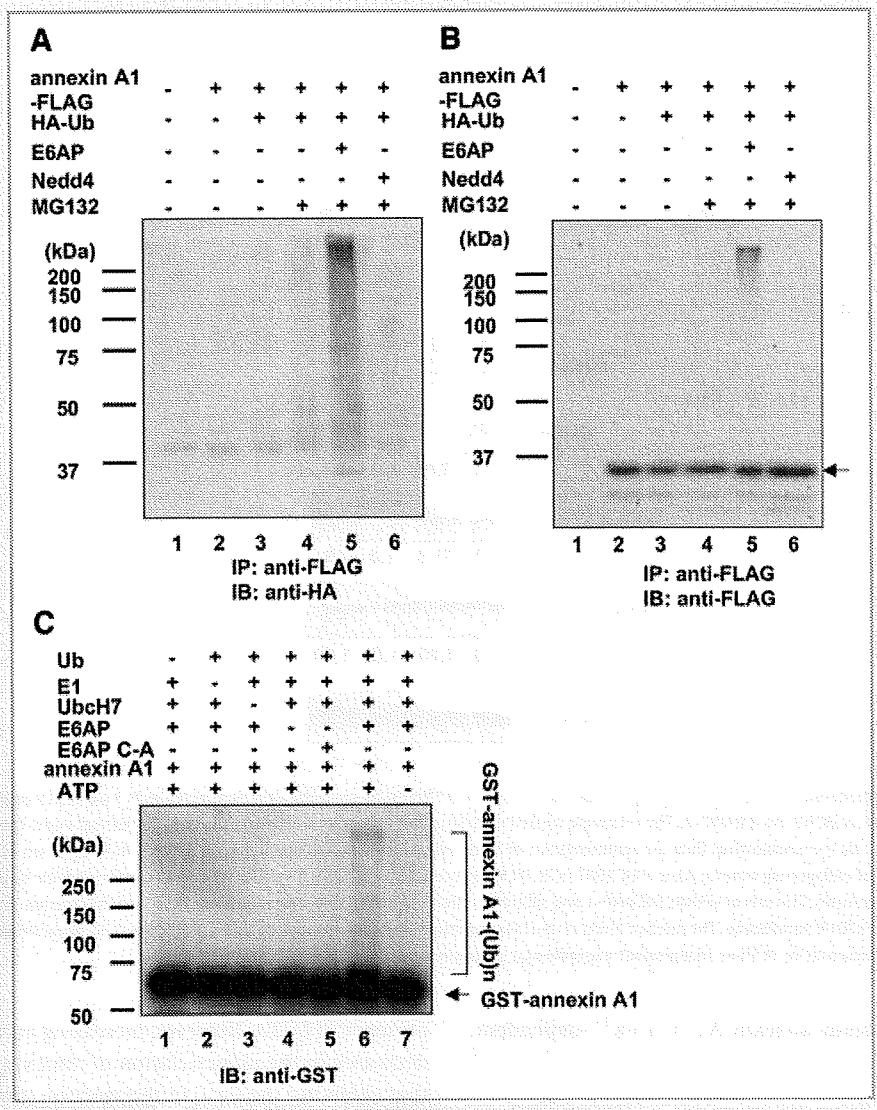

Fig. 5. E6AP-dependent ubiquitylation of annexin A1 protein in vivo and in vitro. HEK 293T cells (1×10^6 cells/10-cm dish) were transfected with 1 μg of pCAG annexin-FLAG together with 2 μg of plasmid encoding E6AP as indicated. Each transfection also included 2 μg of plasmid encoding HA-ubiquitin. The cell lysates were immunoprecipitated with FLAG beads and analyzed by immunoblotting with anti-HA PAb (A) or anti-FLAG PAb (B). The Western blot shows the presence of a ubiquitin smear. The arrow indicates annexin-FLAG. IB, immunoblot; IP, immunoprecipitation. C: In vitro ubiquitylation of annexin A1 by E6AP. For in vitro ubiquitylation of annexin A1 protein, purified GST-annexin A1 was used as a substrate. Assays were done in 40-μl volumes containing each component as indicated. The reaction mixture is described in the Experimental Procedures. The reaction mixture contained 1 mM $CaCl_2$. The reaction was terminated by addition of SDS–PAGE loading buffer and followed by immunoblotting with anti-GST PAb. The arrow indicates GST-annexin A1. Ubiquitylated species of GST-annexin A1 proteins are marked by brackets.

DISCUSSION

In the present study, we have identified annexin A1 as a novel substrate for E6AP using four lines of evidence: (1) E6AP bound to annexin A1 in vivo and in vitro; (2) overexpression of E6AP enhanced proteasomal degradation of annexin A1 in vivo; (3) knockdown of endogenous E6AP by siRNA resulted in the accumulation of endogenous annexin A1 in vivo; and (4) E6AP enhanced the polyubiquitylation of annexin A1 in vivo and in vitro. These results provide evidence that E6AP mediates the ubiquitylation and proteasomal degradation of annexin A1. We have shown that E6AP bound to annexin A1 only in the presence of Ca^{2+} and that these interactions were enhanced by increasing concentrations of Ca^{2+}. Annexin A1 was polyubiquitylated by E6AP only in the presence of Ca^{2+}. Chelating Ca^{2+} with EGTA inhibited E6AP-mediated polyubiquitylation of annexin A1. The E6AP-binding domain on annexin A1 was mapped to the core domain, especially the annexin repeat domain III. These results suggest that the conformational change of annexin A1 induced by Ca^{2+} binding allows E6AP to bind to annexin repeat domain III of annexin A1 and to mediate its ubiquitylation and degradation.

Post-translational modifications, such as Ca^{2+} binding, phosphorylation, and lipidation, have roles in the regulation of annexin A1. Solito et al. [2006] showed that the translocation of annexin A1 from the cytoplasm to the cell surface is regulated by phosphorylation and lipidation. Annexin A1 is phosphorylated by several

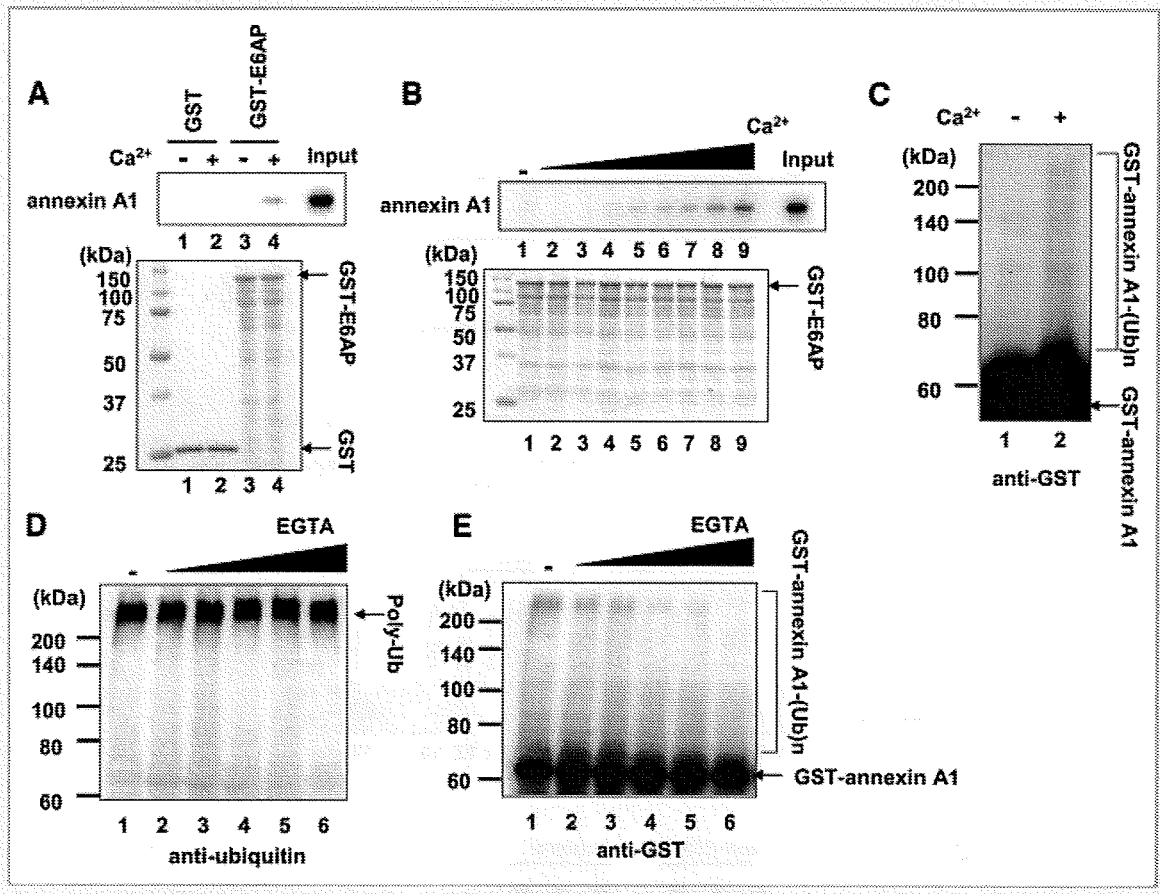

Fig. 6. E6AP mediates ubiquitylation of annexin A1 in a Ca^{2+}-dependent manner. A: In vitro binding of annexin A1 and E6AP. Immobilized GST-E6AP or GST alone was incubated with purified His-annexin A1 in the presence or absence of 1 mM $CaCl_2$ in the binding solution. Immunoblotting to detect bound annexin A1 was performed using anti-annexin A1 antibody. B: Ca^{2+}-dependent interaction between annexin A1 and E6AP. The GST pull-down assays described in (A) were repeated in the presence of increasing concentrations of $CaCl_2$ in the binding solution as follows: lane 1 (0 μM), 2 (10 μM), 3 (100 μM), 4 (250 μM), 5 (500 μM), 6 (750 μM), 7 (1 mM), 8 (2.5 mM), and 9 (5 mM). C: For in vitro ubiquitylation of annexin A1 protein, purified GST-annexin A1 was used as a substrate. Assays were done in 40-μl volumes in the presence or absence of 1 mM $CaCl_2$. The reaction mixture is described in Materials and Methods Section. The reaction was terminated by addition of SDS–PAGE loading buffer and followed by immunoblotting with anti-GST PAb. Arrow indicates GST-annexin A1. Ubiquitylated species of GST-annexin A1 proteins are marked by brackets. D,E: The in vitro ubiquitylation assays were performed in the presence of various concentrations of EGTA in the reaction mixture containing 1 mM $CaCl_2$. The concentrations of EGTA were as follows: lane 1 (0 mM), 2 (0.1 mM), 3 (0.5 mM), 4 (1 mM), 5 (5 mM), and 6 (10 mM). D: Immunoblotting to detect whole polyubiquitylated proteins with anti-ubiquitin MAb. E: Immunoblotting to detect polyubiquitylated GST-annexin A1 with anti-GST PAb.

protein kinases, such as epidermal growth factor receptor protein kinase, protein kinase C, and hepatocyte growth factor receptor kinase to mediate proliferation [Lim and Pervaiz, 2007], suggesting that phosphorylation plays some roles in the regulation of annexin A1 function. The findings presented in this study suggest that the ubiquitin-proteasome pathway plays a role in the regulation of annexin A1 function. Our data also suggest that E6AP preferentially recognizes the Ca^{2+}-binding form of annexin A1 and targets it for proteasomal degradation. The main biological property of annexin A1 is the binding to the phospholipid membrane in a Ca^{2+}-dependent manner [Lim and Pervaiz, 2007]. X-ray crystallography studies of annexin A1 have suggested that a calcium-driven conformational switch of the N-terminal and core domains of annexin A1 involves the membrane aggregation properties of annexin A1 [Rosengarth et al., 2001; Rosengarth and Luecke, 2003]. It will be intriguing to examine the role of E6AP in membrane aggregation. Further investigations will be required to elucidate the role of E6AP in the regulation of annexin A1 functions.

Targeting of a substrate via the ubiquitin system involves specific binding of the protein to the appropriate E3 ubiquitin ligase. There are several modes for specific substrate recognition, such as (1) NH2-terminal residue (N-end rule pathway), (2) allosteric activation, (3) recognition of phosphorylated substrate, (4) phosphorylation of E3, (5) phosphorylation of both the ligase and its substrate, (6) recognition in trans via an ancillary protein, (7) abnormal/mutated/misfolded proteins, and (8) recognition via hydroxylated proline [Glickman and Ciechanover, 2002]. E6AP specifically recognizes active forms of Blk, indicating that tyrosine phosphorylation of the regulatory tyrosine of Blk plays a role in specific substrate recognition [Oda et al., 1999]. Here we propose a novel mechanism of specific substrate recognition in the ubiquitin system, in which E6AP recognizes annexin A1 via a Ca^{2+}-induced conformational change. E6AP plays a direct catalytic role in the

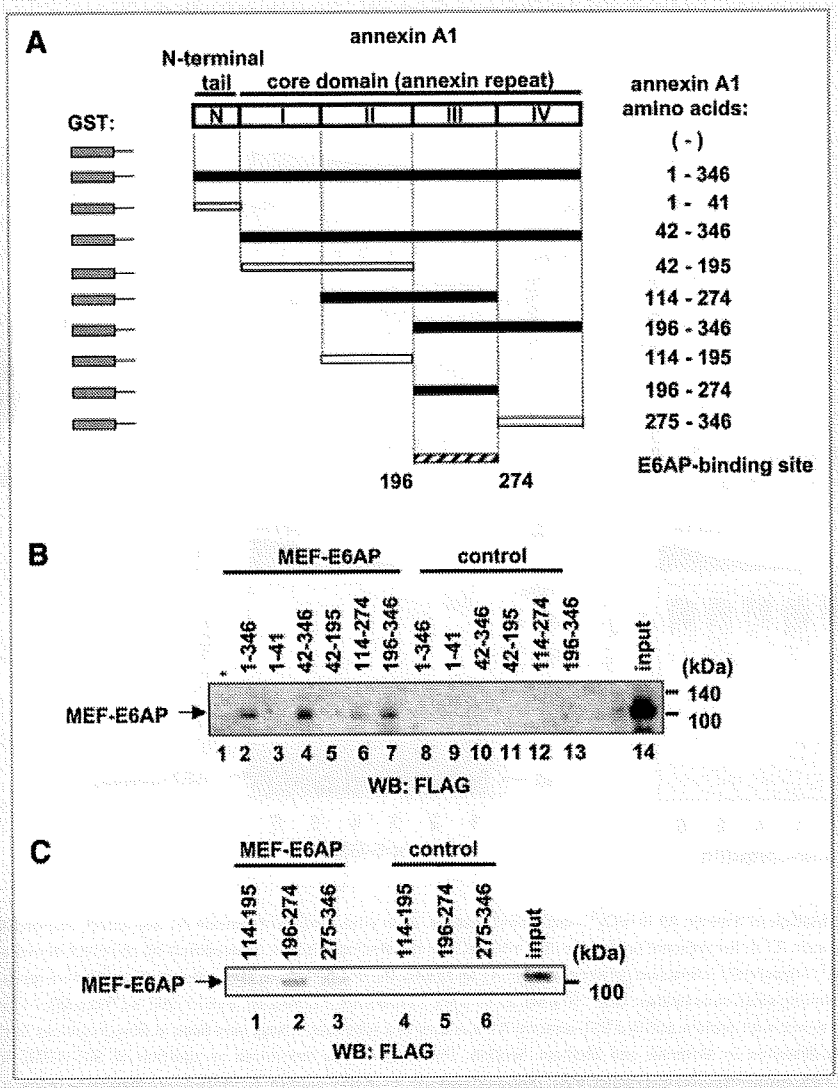

Fig. 7. Mapping of the E6AP-binding domain for annexin A1 protein. A: Structure of annexin A1. Shown is a schematic representation of the region of annexin A1 protein. N-terminal tail (aa 1–41), core domain (aa 42–346), and annexin repeat domains I (aa 42–113), II (aa 114–195), III (aa 196–274), and IV (aa 275–346) are shown. Schematic representation of GST-annexin A1 proteins. GST proteins contain the annexin A1 amino acids indicated to the right. The shaded box in each represents the GST sequence. Closed boxes represent proteins that are bound specifically to MEF-E6AP, and open boxes represent those that are not bound. B,C: In vitro binding of MEF-E6AP to GST-annexin A1 proteins. Purified recombinant MEF-E6AP was assayed for association with GST (–) or the GST-annexin A1 proteins using the binding buffer with 1 mM $CaCl_2$. GST pull-down was performed to assay for the association of E6AP with annexin A1. Control experiments were performed without MEF-E6AP. The association of MEF-E6AP was detected by immunoblotting with anti-FLAG MAb.

final attachment of ubiquitin to substrate proteins. Our findings suggest that Ca^{2+}-induced conformational change of annexin A1 may function as a degradation signal for annexin A1.

Ubiquitylated annexin A2 is enriched in the cytoskeleton fraction of mouse Krebs II cells [Lauvrak et al., 2005]. It remains unclear whether the ubiquitylated annexin A2 is degraded by proteasome. The apical membrane localization of Nedd4, a member of HECT-type ubiquitin ligases, is mediated by an association of its C2 domain with the apically targeted annexin XIIIb [Plant et al., 2000]. However, it is unknown whether annexin XIIIb is a substrate of Nedd4. To our knowledge, this is the first study to identify a specific E3 ubiquitin ligase for the ubiquitylation of an annexin family protein. All annexins share a core domain composed of four similar repeats, each approximately 70 amino acids long. Each repeat is composed of five α helices and usually contains a characteristic type-2 motif for binding calcium ions with the sequence GxGT-[38 residues]-D/E [Moss and Morgan, 2004]. The core domains of most vertebrate annexins reveal conservation of their secondary and tertiary structures despite the presence of only 45–55% amino-acid identity among individual annexins [Moss and Morgan, 2004]. It will be required to investigate whether other annexins are regulated by E6AP or other E3 ubiquitin ligases.

E6AP is hijacked by the HPV16E6 to target the tumor suppressor p53 in cervical cancer. Moreover, E6AP is mutated in Angelman syndrome and mediates ubiquitin-dependent degradation of HCV core protein, suggesting that E6AP plays important roles in sporadic and hereditary human diseases including cancer, neurological disorders, and infectious diseases [Kishino et al., 1997; Scheffner

and Staub, 2007; Shirakura et al., 2007]. Physical and functional association of E6AP with viral proteins, such as HPV16E6 [Huibregtse et al., 1993b] and HCV core protein [Shirakura et al., 2007], have been demonstrated. It is possible that the viral proteins redirect E6AP away from annexin A1, increasing the stability of annexin A1, and thereby contributing to viral pathogenesis. It would be interesting to investigate whether these viral proteins affect E6AP-dependent degradation of annexin A1. The association of E6AP with the viral protein (HPV16E6 or HCV core protein) could provide a feasible target for molecular approaches in the treatment of cervical cancer or HCV-related diseases.

In conclusion, we have demonstrated that E6AP interacts with annexin A1 protein and mediates its ubiquitin-dependent degradation. We propose that E6AP may play a role in regulating the diverse functions of annexin A1 protein. Identification of the specific E3 ubiquitin ligase may provide a link between the annexin family proteins and the ubiquitin-proteasome pathway. Elucidating the regulation of annexin A1 may provide a novel clue in the treatment of the E6AP-related diseases.

ACKNOWLEDGMENTS

We thank Dr. Bohmann (EMBL) for providing pMT123 and Dr. Iwai (Osaka University) for recombinant baculovirus carrying His_6-mouse E1. We also thank S. Yoshizaki, M. Ikeda, and M. Sasaki for technical assistance, and T. Mizoguchi and K. Hachida for secretarial work. This work was supported in part by a grant for Research on Health Sciences focusing on Drug Innovation from the Japan Health Sciences Foundation; by grants-in-aid from the Ministry of Health, Labor, and Welfare; and by the program for Promotion of Fundamental Studies in Health Sciences of the National Institute of Biomedical Innovation (NIBIO), Japan.

REFERENCES

Buckingham JC, John CD, Solito E, Tierney T, Flower RJ, Christian H, Morris J. 2006. Annexin 1, glucocorticoids, and the neuroendocrine-immune interface. Ann NY Acad Sci 1088:396–409.

Ciechanover A. 1998. The ubiquitin-proteasome pathway: On protein death and cell life. EMBO J 17:7151–7160.

Ciechanover A, Heller H, Katz-Etzion R, Hershko A. 1981. Activation of the heat-stable polypeptide of the ATP-dependent proteolytic system. Proc Natl Acad Sci USA 78:761–765.

Ciechanover A, Orian A, Schwartz AL. 2000. Ubiquitin-mediated proteolysis: Biological regulation via destruction. Bioessays 22:442–451.

Cooper EM, Hudson AW, Amos J, Wagstaff J, Howley PM. 2004. Biochemical analysis of Angelman syndrome-associated mutations in the E3 ubiquitin ligase E6-associated protein. J Biol Chem 279:41208–41217.

Gewin L, Myers H, Kiyono T, Galloway DA. 2004. Identification of a novel telomerase repressor that interacts with the human papillomavirus type-16 E6/E6-AP complex. Genes Dev 18:2269–2282.

Glickman MH, Ciechanover A. 2002. The ubiquitin-proteasome proteolytic pathway: Destruction for the sake of construction. Physiol Rev 82:373–428.

Haas AL, Rose IA. 1982. The mechanism of ubiquitin activating enzyme. A kinetic and equilibrium analysis. J Biol Chem 257:10329–10337.

Haigler HT, Schlaepfer DD, Burgess WH. 1987. Characterization of lipocortin I and an immunologically unrelated 33-kDa protein as epidermal growth factor receptor/kinase substrates and phospholipase A2 inhibitors. J Biol Chem 262:6921–6930.

Harris KF, Shoji I, Cooper EM, Kumar S, Oda H, Howley PM. 1999. Ubiquitin-mediated degradation of active Src tyrosine kinase. Proc Natl Acad Sci USA 96:13738–13743.

Hershko A, Ciechanover A. 1998. The ubiquitin system. Annu Rev Biochem 67:425–479.

Hershko A, Heller H, Eytan E, Reiss Y. 1986. The protein substrate binding site of the ubiquitin-protein ligase system. J Biol Chem 261:11992–11999.

Huibregtse JM, Scheffner M, Howley PM. 1993a. Cloning and expression of the cDNA for E6-AP, a protein that mediates the interaction of the human papillomavirus E6 oncoprotein with p53. Mol Cell Biol 13:775–784.

Huibregtse JM, Scheffner M, Howley PM. 1993b. Localization of the E6-AP regions that direct human papillomavirus E6 binding, association with p53, and ubiquitination of associated proteins. Mol Cell Biol 13:4918–4927.

Huibregtse JM, Scheffner M, Beaudenon S, Howley PM. 1995. A family of proteins structurally and functionally related to the E6-AP ubiquitin-protein ligase. Proc Natl Acad Sci USA 92:2563–2567.

Kaji H, Tsuji T, Mawuenyega KG, Wakamiya A, Taoka M, Isobe T. 2000. Profiling of Caenorhabditis elegans proteins using two-dimensional gel electrophoresis and matrix assisted laser desorption/ionization-time of flight-mass spectrometry. Electrophoresis 21:1755–1765.

Kao WH, Beaudenon SL, Talis AL, Huibregtse JM, Howley PM. 2000. Human papillomavirus type 16 E6 induces self-ubiquitination of the E6AP ubiquitin-protein ligase. J Virol 74:6408–6417.

Kelley ML, Keiger KE, Lee CJ, Huibregtse JM. 2005. The global transcriptional effects of the human papillomavirus E6 protein in cervical carcinoma cell lines are mediated by the E6AP ubiquitin ligase. J Virol 79:3737–3747.

Kishino T, Lalande M, Wagstaff J. 1997. UBE3A/E6-AP mutations cause Angelman syndrome. Nat Genet 15:70–73.

Kuhne C, Banks L. 1998. E3-ubiquitin ligase/E6-AP links multicopy maintenance protein 7 to the ubiquitination pathway by a novel motif, the L2G box. J Biol Chem 273:34302–34309.

Kumar S, Talis AL, Howley PM. 1999. Identification of HHR23A as a substrate for E6-associated protein-mediated ubiquitination. J Biol Chem 274:18785–18792.

Lauvrak SU, Hollas H, Doskeland AP, Aukrust I, Flatmark T, Vedeler A. 2005. Ubiquitinated annexin A2 is enriched in the cytoskeleton fraction. FEBS Lett 579:203–206.

Lim LH, Pervaiz S. 2007. Annexin 1: The new face of an old molecule. FASEB J 21:968–975.

Mani A, Oh AS, Bowden ET, Lahusen T, Lorick KL, Weissman AM, Schlegel R, Wellstein A, Riegel AT. 2006. E6AP mediates regulated proteasomal degradation of the nuclear receptor coactivator amplified in breast cancer 1 in immortalized cells. Cancer Res 66:8680–8686.

Moss SE, Morgan RO. 2004. The annexins. Genome Biol 5:219.

Nakagawa S, Huibregtse JM. 2000. Human scribble (Vartul) is targeted for ubiquitin-mediated degradation by the high-risk papillomavirus E6 proteins and the E6AP ubiquitin-protein ligase. Mol Cell Biol 20:8244–8253.

Niwa H, Yamamura K, Miyazaki J. 1991. Efficient selection for high-expression transfectants with a novel eukaryotic vector. Gene 108:193–199.

Oda H, Kumar S, Howley PM. 1999. Regulation of the Src family tyrosine kinase Blk through E6AP-mediated ubiquitination. Proc Natl Acad Sci USA 96:9557–9562.

Oudinet JP, Russo-Marie F, Cavadore JC, Rothhut B. 1993. Protein kinase C-dependent phosphorylation of annexins I and II in mesangial cells. Biochem J 292(Pt 1):63–68.

Plant PJ, Lafont F, Lecat S, Verkade P, Simons K, Rotin D. 2000. Apical membrane targeting of Nedd4 is mediated by an association of its C2 domain with annexin XIIIb. J Cell Biol 149:1473–1484.

Rosengarth A, Luecke H. 2003. A calcium-driven conformational switch of the N-terminal and core domains of annexin A1. J Mol Biol 326:1317–1325.